Theory of four-wave mixing using an amplitude approach

B. Dubetsky and P. R. Berman
Physics Department, New York University, 4 Washington Place, New York, New York 10003
(Received 18 August 1992)

A theory of four-wave mixing is developed using an amplitude approach in the Schrödinger picture. It is shown that the four-wave mixing signal produced when three fields are incident on an ensemble of two-level atoms can be viewed as arising from constructive interference of the signals emitted at the various atomic sites. Fourteen distinct amplitudes contribute to the four-wave mixing signal. Some of these amplitudes involve final states in which one or two atoms are excited, and some involve final states in which photons are emitted into modes other than a phase-matched mode of interest. The amplitude approach has the advantage of clearly showing the atom-field correlations. It helps one to understand the underlying physical mechanisms responsible for creation of the four-wave mixing signal, as well as features in the line shape resulting from collisions and effects relating to atomic recoil on the absorption or emission of radiation. These so-called collision- and recoil-induced resonances are calculated explicitly using the amplitude approach, and an interpretation of the results in terms of the interference between different amplitudes is given. Our results, calculated for a finite interaction time between the atoms and the fields, are compared with analogous calculations in which an effective ground-state decay time is assumed. It is shown that the results differ if the atom-field interaction time is not the longest relevant time parameter in the problem.

PACS number(s): 32.80.−t, 42.65.−k, 42.50.−p

I. INTRODUCTION

In solving a given problem involving the interaction of radiation with matter, several approaches are generally available. When spontaneous emission plays a nonnegligible role, a density-matrix approach is generally the method of choice. The density-matrix approach may be semiclassical (quantum-mechanical atoms and classical fields) or fully quantized (quantum-mechanical atoms and quantized fields).

In the case of a fully quantized approach, the Heisenberg representation proves to be particularly useful. In the Heisenberg representation one can define separate operators for the atoms and the field. For example, consider a "two-level" atom having levels labeled by 1 and 2 interacting with one or more modes of the radiation field. Atomic operators $\sigma_{ij}=|i\rangle\langle j|$ $(i,j=1,2)$ can be defined which can be related to atomic-state populations and coherences. A simplifying feature of the Heisenberg representation is that these operators contain an implicit trace over all field variables. If one is able to solve for the σ_{ij}'s, then one has, in effect, obtained the reduced density matrix describing the atomic system. It should also be noted that the σ_{ij}'s can satisfy simple operator equations. For example, if the two-level system under investigation is "closed" in the sense that there is no leakage to other levels, then one finds $(\sigma_{11}+\sigma_{22})=1$.

The Heisenberg approach can be used to isolate field variables as well as atomic variables. If one were interested in calculating the number of photons present in a mode $\mathbf{k}$, one need only calculate the operator $n_{\mathbf{k}}=a_{\mathbf{k}}^{\dagger}a_{\mathbf{k}}$, whose expectation value gives the average number of photons in mode $\mathbf{k}$. This operator contains an implicit sum over all atomic variables, enabling one to directly calculate the reduced density matrix for the radiation fields.

When spontaneous emission is present or when one wishes to calculate reduced density-matrix elements for the atoms or the fields, it might seem foolhardy or even impossible to use a state amplitude approach based on the Schrödinger representation. For example, to calculate a reduced density-matrix element ρ_{ij} for the atoms, one must calculate $\sum_{\alpha}b_{i\alpha}b_{j\alpha}^{*}$, where $b_{i\alpha}$ is a probability amplitude and α refers to all states of the field. Similarly, to calculate the number of photons in a mode $\mathbf{k}$ one must calculate $\sum_{i=1,2;\alpha\neq\mathbf{k}}|b_{i\mathbf{k}\alpha}|^2$. In general, the evaluation of all these probability amplitudes represents a horrendous task.

As complicated as the Schrödinger representation appears to be, there *are* some very good reasons to apply it to problems involving the interaction of radiation with matter. In following the Schrödinger approach, any atom-field correlations are clearly revealed in the probability amplitudes. Such correlations are hidden in the Heisenberg approach since the atom and field operators already correspond to reduced density matrices for the atoms and the fields, respectively. Of course, this is precisely what makes the Heisenberg approach ideal for computational purposes. On the other hand, if one wishes to understand the underlying physical mechanisms giving rise to the signal under investigation, the Schrödinger amplitudes provide more information than the Heisenberg operators. Given the difficulty and controversy in explaining the physical origin of such lineshape features as the pressure-induced extra resonances in four-wave mixing [1], it may prove interesting to at-

tack such problems using an amplitude approach.

This method has already been used to analyze the collision-induced resonances in a three-wave mixing scheme involving three-level atoms [2]. It was found that the pressure-induced resonances could be uniquely identified with amplitudes involving the emission of spontaneous photons. Moreover, the interference from different atomic sites giving rise to the signal was clearly evident in the Schrödinger approach. The situation becomes much more complex when one considers four-wave mixing in an ensemble of two-level atoms. In this case, one must properly account for the repopulation of the atomic ground state resulting from spontaneous emission from the excited state.

A geometry for four-wave mixing is shown in Fig. 1. Three fields having wave vectors $\mathbf{k}_1=\mathbf{k}$, $\mathbf{k}_2=-\mathbf{k}$, and $\mathbf{k}_3$ are incident on an atomic medium consisting of two-level atoms. Fields 1 and 2 have frequency Ω, while field 3 has frequency $(\Omega+\delta)$. The four-wave mixing signal intensity in the direction $-\mathbf{k}_3$ is measured as a function of δ. For a closed atomic system there is no resonance in the line shape centered at $\delta=0$, provided that all effects arising from atomic collisions and atomic recoil on the absorption or emission of photons are neglected. Collisions lead to a resonance centered at $\delta=0$ having width of order Γ (excited-state decay rate) [1], while atomic recoil can lead to a resonance centered at $\delta=0$ whose width is given by some effective ground-state width [3].

The physical explanation of the absence of the $\delta=0$ resonance in the absence of collisions and atomic recoil has been the subject of some controversy. The absence of the resonance has been explained as arising from the interference of two chains in a density-matrix calculation [4]. The disappearance has also been explained on the basis of conservation of energy arguments [5].

A fundamental calculation of the four-wave mixing signal based on an amplitude approach might provide new insight into the nature of the origin of the four-wave mixing signal. It is the goal of this article to present such a calculation. The interference of various quantum-mechanical amplitudes giving rise to the disappearance of the $\delta=0$ resonance is clearly apparent in our approach. In Sec. II, a discussion and evaluation of the various amplitudes contributing to the signal is given. The calculation is extended to include effects arising from atomic recoil in Sec. III. This calculation reproduces the results obtained from a density-matrix approach [3], and provides some new insight into the origin of the recoil-induced resonances. Most of the calculations in the main text are carried out in the so-called secular approximation (atom-field detunings large compared with atomic decay rates). The Appendixes contain generalizations of the results valid for arbitrary ratios of detuning to decay rates. Moreover, the line shape corresponding to the collision-induced resonances is derived in Appendix B.

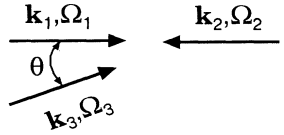

FIG. 1. A geometry for four-wave mixing that can lead to phase-matched emission into a field mode having wave vector $\mathbf{k}=\mathbf{k}_1-\mathbf{k}_3+\mathbf{k}_2$. For some of the illustrative examples in the text, the parameters are chosen such that $\mathbf{k}_1=-\mathbf{k}_2$, $\Omega_1=\Omega_2$, $\Omega_3=\Omega_1+\delta$, and $\theta\ll 1$.

II. STATIONARY ATOMS

A. Qualitative description

Consider the interaction of the three field modes having frequencies $\Omega_1,\Omega_2,\Omega_3$, wave vectors $\mathbf{k}_1,\mathbf{k}_2,\mathbf{k}_3$, and initial photon occupation numbers n_1,n_2,n_3, respectively, with an ensemble of N stationary two-level atoms, each of which is initially in its ground state 1 (see Fig. 2). Coherent emission via four-wave mixing (4WM) can be produced in a new field mode having wave vector

$$\mathbf{k}=\mathbf{k}_1+\mathbf{k}_2-\mathbf{k}_3 \tag{1a}$$

and frequency

$$\Omega_{\mathbf{k}}=\Omega_1+\Omega_2-\Omega_3\ , \tag{1b}$$

provided the phase-matching condition

$$k=\Omega_{\mathbf{k}}/c \tag{1c}$$

is satisfied.

Our goal in this paper is to calculate the 4WM signal using an amplitude approach. We consider only the 4WM into the mode $\mathbf{k}$ given by Eqs. (1). The rate at which photons are emitted into mode $(\mathbf{k},\Omega_{\mathbf{k}})$ can be written

$$I_{\mathbf{k}}=\dot{n}_{\mathbf{k}}=\frac{d}{dt}\sum_{n_1',n_2',n_3',n_\alpha}\left|\sum_{\{i\}}b[\{i\};n_1',n_2',n_3';1_{\mathbf{k}},n_\alpha]\right|^2, \tag{2}$$

where $b[\{i\};n_1',n_2',n_3';1_{\mathbf{k}},n_\alpha]$ is the probability amplitude for finding a photon in mode $\mathbf{k}$, n_i' photons in field i, n_α photons in initially unoccupied field modes other than mode $\mathbf{k}$, and the atoms in some configuration of internal states $\{i\}$.

As an example of an amplitude contributing to emission at $\mathbf{k}=\mathbf{k}_1+\mathbf{k}_2-\mathbf{k}_3$, we consider the amplitude represented schematically in Fig. 3. At each atomic site j, an atom can "absorb" photon 1, "emit" photon 3, "absorb" photon 2, and emit a signal photon $\mathbf{k}$. By summing over all sites j, one arrives at the probability amplitude for all atoms to be in state 1, with the absorption of a photon from each of fields 1 and 2, and emission of a photon in fields 3 and $\mathbf{k}$. The contribution to the sum in Fig. 3 from atom j, located at position $\mathbf{r}_j$, contains a spatial

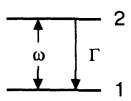

FIG. 2. Energy-level diagram for the "two-level" atoms considered in this work.

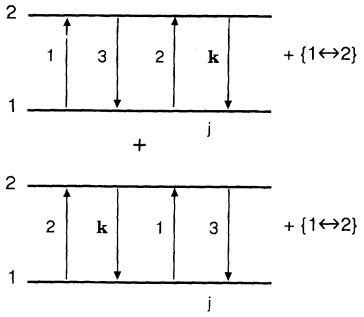

FIG. 3. Schematic representation of the probability amplitude for atom j to absorb a photon from each of fields 1 and 2, and emit a photon into each of fields 3 and $\mathbf{k}$.

phase factor which can be obtained by assigning a factor $\exp(i\mathbf{k}_i\cdot\mathbf{r}_j)$ to each upward arrow i and $\exp(-i\mathbf{k}_i\cdot\mathbf{r}_j)$ to each downward one. The overall phase factor for Fig. 3 is $\exp(i\bar{\mathbf{k}}\cdot\mathbf{r}_j)$, where

$$\bar{\mathbf{k}}=\mathbf{k}_1-\mathbf{k}_3+\mathbf{k}_2-\mathbf{k}\ . \tag{3}$$

As long as the momentum conservation condition $\bar{\mathbf{k}}=\mathbf{0}$ is satisfied, the contributions to the probability amplitude from different atomic sites add in phase. Consequently, the signal intensity, which is proportional to the square of the probability amplitude, varies as the square of the atomic density.

The interactions shown schematically in Fig. 3 are not sufficient to completely characterize the 4WM signal [6]. One must also consider diagrams, such as these shown in Fig. 4, in which some of the fields act at atomic site j and others at site j'. Figure 4 represents an amplitude for all atoms to be in state 1, with the absorption of a photon from each of fields 2 and 3, and emission of a photon into fields 1 and $\mathbf{k}$. For a given pair of atoms (j,j') atom j absorbs photon 2 and emits photon $\mathbf{k}$, and atom j' absorbs photon 3 and emits photon 1. In summing over j and j' and squaring this amplitude one finds terms which vary as

$$\sum_{j,j'}\sum_{l,l'}\exp[i(\mathbf{k}_2-\mathbf{k})\cdot\mathbf{r}_j+i(\mathbf{k}_3-\mathbf{k}_1)\cdot\mathbf{r}_{j'} -i(\mathbf{k}_2-\mathbf{k})\cdot\mathbf{r}_l-i(\mathbf{k}_3-\mathbf{k}_1)\cdot\mathbf{r}_{l'}]$$

For $l=j'$ and $l'=j$ one arrives at a net phase factor $\exp(i\bar{\mathbf{k}}\cdot r_{jj'})$ where $r_{jj'}=\mathbf{r}_j-\mathbf{r}_{j'}$. Under phase-matching conditions, this term results in a coherent contribution to

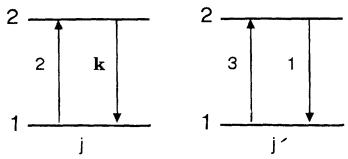

FIG. 4. Schematic representation of the joint probability amplitude for atom j to absorb a photon from field 2 and emit a photon into field $\mathbf{k}$ and for atom j' to absorb a photon from field 3 and emit a photon into field 1.

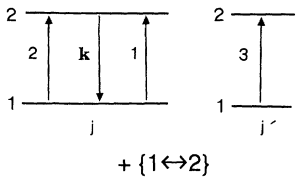

FIG. 5. Schematic representation of the joint probability amplitude for atom j to absorb a photon from each of fields 1 and 2 and emit a photon into field $\mathbf{k}$, and for atom j' to absorb a photon from field 3.

the 4WM signal, proportional to N^2.

It is also possible to get a nonvanishing contribution to the 4WM signal (2) involving final states in which some of the atoms are excited. One such amplitude is represented in Fig. 5, corresponding to absorption of photon from fields 1, 2, and 3, emission into field mode $\mathbf{k}$, and atoms j and j' in state $|2\rangle$ with all remaining atoms in their ground states. On summing over j and j' and squaring this amplitude, one again arrives at a coherent contribution to the 4WM signal.

Finally one must consider processes involving the emission into modes other than 1, 2, 3, or $\mathbf{k}$. In analogy with three-wave mixing problems [2], one constructs diagrams such as that shown Fig. 6, representing the probability amplitude for all atoms to be in state $|1\rangle$ with an absorption of photons from fields 1, 2, and 3 and emission into modes $\mathbf{k}$, $\mathbf{q}$, and $\mathbf{q}'$. On summing over j and j', and squaring this amplitude, one arrives at probability which has terms that are proportional to

$$\sum_{j,j'}\exp[i(\mathbf{k}_1-\mathbf{q}+\mathbf{k}_2-\mathbf{k})\cdot\mathbf{r}_j+i(\mathbf{k}_3-\mathbf{q}')\cdot\mathbf{r}_{j'}] \times\sum_{l,l'}\exp[-i(\mathbf{k}_1-\mathbf{q}'+\mathbf{k}_2-\mathbf{k})\cdot\mathbf{r}_l-i(\mathbf{k}_3-\mathbf{q})\cdot\mathbf{r}_{l'}]\ .$$

For $l=j'$ and $l'=j$, one again finds a coherent contribution to the 4WM signal.

Normally, spontaneous processes need not be considered in describing multiwave mixing in the so-called secular approximation [7], when the frequencies of the incident fields are tuned far from resonance.

$$|\Omega_i-\omega|\gg\Gamma\quad(i=1,2,3)\ , \tag{4}$$

where ω is the 1-2 transition frequency and Γ is decay rate of level 2. We encounter here a new situation.

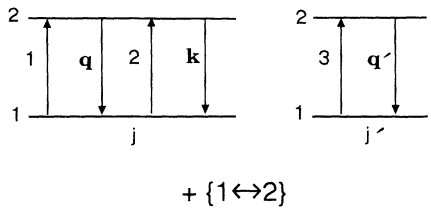

FIG. 6. Schematic representation of the joint probability amplitude for atom j to absorb a photon from each of fields 1 and 2 and emit a photon into each of fields $\mathbf{q}$ and $\mathbf{k}$, and for atom j' to absorb a photon from field 3 and emit a photon into field $\mathbf{q}'$.

Stimulated processes can give rise to signals at a frequency different from that specified in Eq. (1b). Such terms are sensitive to the way in which the fields are turned on and disappear if they are switched on in a time large compared with $[(\Omega_i-\omega)^2+\Gamma^2]^{-1/2}$. If the fields are turned on rapidly, these terms persist; however, it will be seen below that they are exactly canceled by terms arising from processes involving spontaneous emission. Thus, for a consistent treatment of the problem, spontaneous-emission terms must be included.

A method for systematically obtaining all the diagrams corresponding to the relevant probability amplitude for 4WM is given in Appendix A. These diagrams are shown in Fig. 7. By squaring the amplitudes and summing those terms corresponding to phase-matched emission in the direction $\mathbf{k}$, one arrives at the 4WM line shape. It is shown below that the final line shape takes on a remarkably simple form. We note that all calculations are carried out assuming that the number of atoms in a volume equal to k^{-3} is much less than unity. Thus the origin of the N^2 dependence of the signal can be traced to a process similar to that encountered in emission by a phased array of dipoles. There are no collective effects associated with spontaneous emission, as one may encounter in superradiance.

B. Calculation of signal

In this section, the 4WM signal is calculated for a simplified atom-field configuration. The atoms are taken to be stationary and the atom-field detunings $\Delta_i=\Omega_i-\omega$ $(i=1,2,3,\mathbf{k})$ are sufficiently large to satisfy $|\Delta_i|\gg\Gamma$ (secular approximation). The calculation is generalized to allow for moving atoms in the following section and for arbitrary detunings in Appendix B.

We consider the interaction of N stationary atoms with several modes of the radiation field. Initially three modes of the field are occupied, with mode $(\Omega_i,\mathbf{k}_i)$ having occupation number n_i $(i=1,2,3)$. These fields lead to a signal generated into the phase-matched mode $(\Omega_{\mathbf{k}},\mathbf{k})$ and may also lead to radiation in other modes of the field (spontaneous emission). The rate at which photons are produced in the phase-matched mode is calculated to lowest-order perturbation theory in the applied fields. In effect, we must calculate the amplitudes represented schematically in Fig. 7.

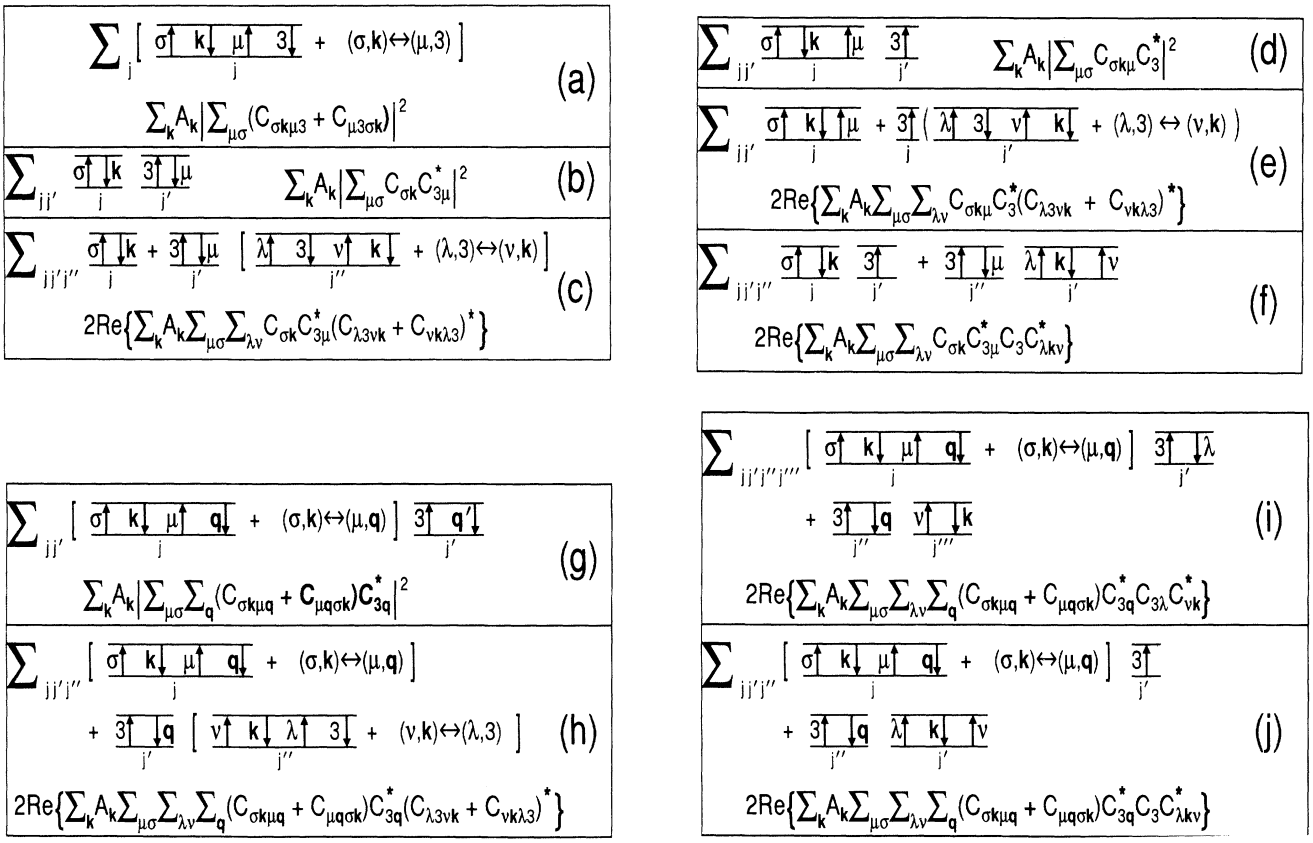

FIG. 7. A schematic representation of all the probability amplitudes that can lead to phase-matched emission in the direction $\mathbf{k}=\mathbf{k}_1-\mathbf{k}_3+\mathbf{k}_2$. The indices μ,σ,ν,λ can be equal to either 1 or 2, with $\mu\neq\sigma,\nu\neq\lambda$. For diagrams (c), (e), (f), and (h)–(j), it is the cross terms in the expression for the probability which contribute. The expressions that result when the amplitudes are squared and the phase-matched contribution retained are also shown in this figure.

In an interaction representation, the Hamiltonian for the atom-field system can be written as

$$H=\sum_{\mu}\sum_{j=1}^{N}\hbar[g_{\mu}S_j^{\dagger}a_{\mu}\exp(i\mathbf{k}_{\mu}\cdot\mathbf{r}_j-i\Delta_{\mu}t) +g_{\mu}^{*}S_j a_{\mu}^{\dagger}\exp(-i\mathbf{k}_{\mu}\cdot\mathbf{r}_j+i\Delta_{\mu}t)] , \quad (5)$$

where $S_j=|1\rangle\langle 2_j|$, $a_i^{\dagger}$ and a_i are creation and destruction operators for mode i, g_{μ} is a coupling coefficient, and

$$\Delta_{\mu}=\Omega_{\mu}-\omega . \quad (6)$$

The ket $|1\rangle$ is shorthand notation for all atoms in their ground states and $|2_j\rangle$ is a shorthand notation for atom j in state 2 and all the other atoms in state 1. Similarly $|2_{ij}\rangle$ would signify that atoms i and j are in state 2 and the remaining atoms in state 1.

Starting from an initial state in which mode i has n_i photons ($i=1,2,3$), all other field modes are empty, and all atoms are in their ground states, one must calculate the probability amplitudes corresponding to Fig. 7. For example, the amplitude needed for Fig. 7(a) is $b(n_1-1,n_2-1,n_3+1,1_{\mathbf{k}})$, implying a final state with all atoms in the ground state, n_1-1 photons in mode 1, n_2-1 photons in mode 2, n_3+1 photons in mode 3, and one photon in mode $\mathbf{k}$. Similarly, the amplitude corresponding to Fig. 7(d) is $b(2_{jj'};n_1-1,n_2-1,n_3-1,1_{\mathbf{k}})$ and that to Fig. 7(i) is $b(n_1,n_2-1,n_3-1,1_{\mathbf{k}},1_{\mathbf{q}})$ for $\lambda=\sigma=1$. The other needed amplitudes can be obtained from the remaining diagrams in Fig. 7. Evolution equations for each of the amplitudes can be derived using the Hamiltonian (5), but it is easier to use the diagrams of Figs. 3–7, together with a few simple rules, to obtain the final state amplitudes.

To each "up" arrow μ ($\mu=1,2,3$), one assigns an integral operator

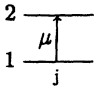

$$\Longrightarrow -i\chi_{\mu}e^{i\mathbf{k}_{\mu}\cdot\mathbf{r}_j}\times\int_0^t dt_1\exp[-i\Delta_{\mu}t_1-\gamma(t-t_1)] , \quad (7a)$$

to each "down" arrow μ ($\mu=1,2,3$), one assigns the integral operator

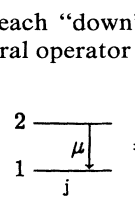

$$\Longrightarrow -i\chi_{\mu}^{*}e^{-i\mathbf{k}_{\mu}\cdot\mathbf{r}_j}\int_0^t dt_1\exp[i\Delta_{\mu}t_1] \quad (7b)$$

and to each down arrow $\mathbf{k}$, one assigns the integral operator

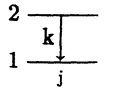

$$\Longrightarrow -ig_{\mathbf{k}}^{*}e^{-i\mathbf{k}\cdot\mathbf{r}_j}\int_0^1 dt_1\exp[i\Delta_{\mathbf{k}}t_1] , \quad (7c)$$

where

$$\gamma=\Gamma/2 \quad (8)$$

and

$$\chi_{\mu}=\sqrt{n_{\mu}}g_{\mu} \quad (9)$$

is a Rabi frequency. It is assumed that $n_{\mu}\gg 1$. The same operator (7c) applies for a down arrow $\mathbf{q}$, with $\mathbf{q}$ replacing $\mathbf{k}$. It should be noted that spontaneous decay is treated exactly (to within the Weisskopf-Wigner approximation) in our calculations, regardless of whether or not the secular approximation is employed. Repopulation of the ground state is rigorously accounted for by terms of type (7c).

By combining these factors, one can easily construct each of the amplitudes in Figs. 3–7. For example, the amplitude corresponding to the first diagram in Fig. 3 is equal to $\sum_j e^{i\bar{\mathbf{k}}\cdot\mathbf{r}_j}C_{132\mathbf{k}}$, where

$$C_{132\mathbf{k}}=\chi_1\chi_3^{*}\chi_2 g_{\mathbf{k}}^{*}\int_0^t dt_1\exp(i\Delta_{\mathbf{k}}t_1)\int_0^{t_1}dt_2\exp[-i\Delta_2 t_2-\gamma(t_1-t_2)] \times\int_0^{t_2}dt_3\exp(i\Delta_3 t_3)\int_0^{t_3}dt_4\exp[-i\Delta_1 t_4-\gamma(t_3-t_4)] , \quad (10)$$

and $\bar{\mathbf{k}}=\mathbf{k}_1-\mathbf{k}_3+\mathbf{k}_2-\mathbf{k}$. In this notation C_{abcd} refers to a diagram in which mode a is absorbed, b emitted, c absorbed, and d emitted. To get the total probability for 4WM in the direction $\mathbf{k}$, one squares each of the amplitudes in Fig. 7, sums these squares and retains only those terms varying as

$$A_{\mathbf{k}}=\sum_{i=1}^{N}\sum_{j=1}^{N}\exp[i\bar{\mathbf{k}}\cdot(\mathbf{r}_i-\mathbf{r}_j)] , \quad (11)$$

which lead to coherent, phase-matched emission in the direction $\mathbf{k}=\mathbf{k}_1-\mathbf{k}_3+\mathbf{k}_2$.

By carrying out this procedure, one arrives at an emission probability given by

$$P=\sum_{\mathbf{k}}A_{\mathbf{k}}\left|\left[C^{\mathrm{st}}+C^{\mathrm{sp}}\right]\right|^2 , \quad (12a)$$

where

$$C^{\mathrm{st}}=\sum_{\substack{\mu,\sigma=1\\ \mu\neq\sigma}}^{2} C^{\mathrm{st}}(\mu,\sigma), C^{\mathrm{sp}}=\sum_{\substack{\mu,\sigma=1\\ \mu\neq\sigma}}^{2} C^{\mathrm{sp}}(\mu,\sigma)\ , \tag{12b}$$

$$C^{\mathrm{st}}(\mu,\sigma)=C_{\mu 3\sigma\mathbf{k}}+C_{\sigma\mathbf{k}\mu 3}+C_3^* C_{\sigma\mathbf{k}\mu}+C_{\sigma\mathbf{k}}C_{3\mu}^*\ , \tag{12c}$$

and

$$C^{\mathrm{sp}}(\mu,\sigma)=\sum_{\mathbf{q}}(C_{\mu\mathbf{q}\sigma\mathbf{k}}+C_{\sigma\mathbf{k}\mu q})C_{3\mathbf{q}}^*\ . \tag{12d}$$

The sum over $\mathbf{k}$ is over a small range in the phase-matched direction. The two summands in the square brackets of (12a) reflect the role of purely stimulated processes and those accompanied by spontaneous emission. We shall refer to $[C^{\mathrm{st}}(\mu,\sigma)$ and $C^{\mathrm{st}}]$ as "stimulated" amplitudes and $[C^{\mathrm{sp}}(\mu,\sigma)$ and $C^{\mathrm{sp}}]$ as "spontaneous" amplitudes, respectively. The amplitudes $C^{\mathrm{st}}(\mu,\sigma)$ and $C^{\mathrm{sp}}(\mu,\sigma)$ $[(\mu,\sigma=1,2;\ \mu\neq\sigma]$ can be viewed as arising from the scattering of field σ from the spatial atomic grating formed in the medium by fields 3 and μ. Note that the final expression for the 4WM line shape has simplified considerably. It has been reduced to the square of the sum of a few terms rather than the sum of the squares of many terms.

It is a rather straightforward matter to calculate the various C factors appearing in Eqs. (12) using the rules (7). Before doing so, however, it is interesting to anticipate the qualitative form of the results. Consider the limit in which $\Delta_1\simeq\Delta_2\simeq\Delta_3\simeq\Delta_{\mathbf{k}}\simeq\Delta$ and $|\Delta|\gg\gamma$. In looking at a C factor such as $C_{132\mathbf{k}}$, one might conclude that the probability amplitude for 4WM varies as

$$\chi_1\chi_3^*\chi_2 g_{\mathbf{k}}^*(t^2/\Delta^2)\ ,$$

where each Δ^{-1} factor arises from the detuning of the up arrows from the 1-2 transition frequency and each t factor arises from the nearly resonant multiphoton interactions terminating on the ground state (there are two such processes in the $C_{132\mathbf{k}}$ diagram). It is clear that this term cannot be the leading term in the 4WM amplitude since it will not give rise to a linear t dependence for the total probability for 4WM. There must be a cancellation of this term when all contributions to the signal are included, such that the leading term will vary as (t/Δ^3). This is reminiscent of the result using a density-matrix approach, in which any resonances characterized by an effective ground state width do not appear if the total population $(\rho_{11}+\rho_{22})$ is conserved [8]. As we shall see, this result is modified when effects related to atomic recoil are included.

We first calculate the stimulated amplitude (12b) using the rules (7). Each of the C parameters needed for the evaluation of C^{st} are calculated in the limit

$$t\gg\gamma^{-1}\gg|\Delta_i|^{-1}(i=1,2,3,\mathbf{k})\ . \tag{13}$$

For example, one finds

$$C_3=(\chi_3/\Delta_3)\exp(-i\Delta_3 t)\ , \tag{14a}$$

$$C_{31}=-i(\chi_3\chi_1^*/\Delta_3)[\xi(\Delta_{13})-i/\Delta_1]\ , \tag{14b}$$

$$C_{1\mathbf{k}2}=-i\chi_1 g_{\mathbf{k}}^*\chi_2(\Delta_1\Delta_2)^{-1}\exp(-i\Delta_2 t)\xi(\Delta_{\mathbf{k}1})\ , \tag{14c}$$

$$\begin{aligned}C_{132\mathbf{k}}=&-\chi_1\chi_3^*\chi_2 g_{\mathbf{k}}^*(\Delta_1\Delta_2)^{-1}\\ &\times[\xi(\Delta_{\mathbf{k}2},\Delta_{31})-i(\Delta_1+\Delta_2-\Delta_3)^{-1}\\ &\times\xi(\bar{\Delta})-i\Delta_3^{-1}\xi(\Delta_{\mathbf{k}2})]\ ,\end{aligned} \tag{14d}$$

where

$$\xi(x)=\int_0^t dt_1\exp(ixt_1)\ , \tag{15a}$$

$$\xi(\Delta,\Delta')=\int_0^t dt_1 e^{i\Delta t_1}\int_0^{t_1} dt_2 e^{i\Delta' t_2}\ , \tag{15b}$$

$$\Delta_{ij}=\Delta_i-\Delta_j\ , \tag{16}$$

and

$$\bar{\Delta}=\Delta_{\mathbf{k}}+\Delta_3-\Delta_1-\Delta_2\ . \tag{17}$$

In the expression for $C_{132\mathbf{k}}$, time-independent terms, which ultimately would not contribute to the 4WM signal, have been omitted.

Equations (14), with various permutations of the indices, are sufficient for calculating the stimulated amplitude. Combining these terms according to (12b) and using the fact that

$$\xi(\Delta,\Delta')+\xi(\Delta',\Delta)=\xi(\Delta)\xi(\Delta')\ , \tag{18}$$

one can obtain

$$C^{\mathrm{st}}(\mu,\sigma)=i\chi_1\chi_3^*\chi_2 g_{\mathbf{k}}^*(\Delta_1\Delta_2)^{-1}\{\xi(\bar{\Delta})[(\Delta_1+\Delta_2-\Delta_3)^{-1}+(\Delta_1+\Delta_2-\Delta_{\mathbf{k}})^{-1}]+\Delta_3^{-1}\xi(\Delta_{\mathbf{k}\sigma})+\Delta_{3\mu}(\Delta_{\mathbf{k}}\Delta_3)^{-1}\xi(\Delta_{3\mu})\}\ . \tag{19}$$

The notation implicit in Eq. (19), and to be used unless indicated otherwise, is that the indices μ and σ appearing in expressions for probability amplitudes take on the values 1 or 2 with $\mu\neq\sigma$. The following points can be noted with regard to the stimulated amplitude. (i) The last term in the curly braces should be dropped since it is of order $(|\Delta|t)^{-1}\ll 1$ times smaller than the other terms. (ii) The $\xi(\bar{\Delta})$ function in the first term defines the frequency of emission as $\Omega_{\mathbf{k}}=\Omega_1-\Omega_3+\Omega_2$ to within a spread of photon energies given by $\delta E_{\mathbf{k}}\sim\hbar/t$. This term corresponds to 4WM under the phase-matching conditions given in Eq. (1). As was noted above, all contribution of order Δ^{-2} have canceled in the final result (19). (iii) The second term corresponds to emission at frequency $\Omega_{\mathbf{k}}=\Omega_\sigma$ and could, in principle, be phase-matched if $\Omega_\sigma=kc$. It is shown below, however, that this term is canceled by the spontaneous amplitude. (iv) While hidden in the final result, the contribution to the stimulated amplitude corresponding to $C_3^* C_{2\mathbf{k}1}$ makes a non-negligible contribution. Owing to a resonance condition involving the up 2 and down $\mathbf{k}$ arrows in Figs. 7(d)–7(f) it is possible to get a contribution from final states involving

excited atoms that is still linear in time.

We now turn to the spontaneous amplitude,

$$C^{\mathrm{sp}}(\mu,\sigma)=\sum_{q}(C_{\mu\mathbf{q}\sigma\mathbf{k}}+C_{\sigma\mathbf{k}\mu\mathbf{q}})C^{*}_{3\mathbf{q}} .$$

In principle, one can use the amplitudes (14), with an appropriate change of indices to calculate the spontaneous amplitude. There is one problem, however. Since there is no restriction put on the detuning $\Delta_{\mathbf{q}}$ one cannot assume that $|\Delta_{\mathbf{q}}|\gg\gamma$. Expressions for the C parameters derived in Appendix B without restriction on values for the detunings can be used. The resulting expression for $C^{\mathrm{sp}}(\mu,\sigma)$, obtained from Eq. (B4), is [9]

$$C^{\mathrm{sp}}(\mu,\sigma)=-i\chi_1\chi_3^{*}\chi_2 g_{\mathbf{k}}^{*}(\Delta_1\Delta_2\Delta_3)^{-1}\xi(\Delta_{\mathbf{k}\sigma}) , \tag{20}$$

assuming that $|\Delta_i|\gg\gamma$ $(i=1,2,3,\mathbf{k})$. This term exactly cancels the second term in the curly braces of (19). Consequently, there is no coherent signal emitted having $\Omega_{\mathbf{k}}=\Omega_{\mu}$ $(\mu=1,2)$. In our amplitude approach, the role of spontaneous emission is clearly isolated, in contrast to calculations carried out using either a semiclassical density matrix [1] or Heisenberg operator approach [10].

It may seem surprising that the spontaneous terms play a non-negligible role in the secular limit $|\Delta_i|\gg\gamma$ $(i=1,2,3,\mathbf{k})$. A complete analysis shows that the spontaneous term, as well as the second term in the curly braces of Eq. (19), is an artifact of the rapid turn-on of the fields. If the fields are turned on smoothly (in a time less than $|\Delta|^{-1}$), the contribution from both of these terms becomes negligible.

Substituting expressions (19) and (20) into Eqs. (12b) and (12a), one obtains a probability

$$P=\left|\frac{2\chi_1\chi_2\chi_3}{\Delta_1\Delta_2\Delta_3}(1+\Delta_3/\Delta_{\mathbf{k}})\right|^2\sum_{\mathbf{k}}A_{\mathbf{k}}|g_{\mathbf{k}}|^2|\xi(\bar{\Delta})|^2 , \tag{21}$$

where the fact that the $|\xi(\bar{\Delta})|^2$ function restricts values of $\Delta\mathbf{k}$ to the vicinity of $\Delta_{\mathbf{k}}=\Delta_1-\Delta_3+\Delta_2$ has been used. The rate of emission $I=\dot{P}$ can be obtained in a manner similar to that used for three-wave mixing [2]. After carrying out the sum over $\mathbf{k}$, one obtains

$$I=I_0\left|2\frac{\chi_1\chi_2\chi_3}{\Delta_1\Delta_2\Delta_3}(1+\Delta_3/\Delta_{\mathbf{k}})\right|^2 , \tag{22}$$

where

$$I_0=\frac{N^2}{S}\frac{2\pi\Omega_{\mathbf{k}}}{\hbar c}|(\mathbf{d}\cdot u_{\mathbf{k}})_{21}|^2 , \tag{23}$$

$\mathbf{u}_{\mathbf{k}}$ is a unit polarization vector for the emitted field and S is the cross-section area of the atom-field interaction volume. This rate agrees with the rate calculated using either a semiclassical [1] or quantized dressed-atom approach [10].

A generalization of this theory to allow for arbitrary ratios of γ to Δ_i is given in Appendix B. Modifications of the line shape resulting from collisions is also analyzed in Appendix B.

III. RECOIL-INDUCED RESONANCES

A. Basic theory

The results of the preceding section can be generalized to a gas of classically moving atoms if the replacement

$$\Delta_i\rightarrow\tilde{\Delta}_i=\Delta_i-\mathbf{k}_i\cdot\mathbf{p}/m \tag{24}$$

is made, where m and $\mathbf{p}$ are the atomic mass and momentum, respectively. In this section, however, we wish to use the amplitude approach to investigate a new class of resonances, the so-called recoil-induced resonances (RIR) [3]. To do so requires a quantization of the atoms' center-of-mass motion. Our approach represents an *entirely quantum treatment,* in which both the fields' and atoms' degrees of freedom are quantized.

The Hamiltonian is conveniently expanded in a momentum-state basis using the fact that $\exp(\pm i\mathbf{k}\cdot\mathbf{r}_j)|\mathbf{p}_j\rangle=|\mathbf{p}_j\pm\hbar\mathbf{k}\rangle$. In an interaction representation, the Hamiltonian for the system of N atoms can be written as

$$H=\sum_{\mu}\sum_{j=1}^{N}\sum_{p_1}\cdots\sum_{\mathbf{p}_N}\hbar\{g_{\mu}S^{\dagger}_{j,\mathbf{p}_j+\hbar\mathbf{k}_{\mu},\mathbf{k}_{\mu}}a_{\mu}\exp[-i(\Delta_{\mu}+\omega_{\mathbf{p}_j,\mathbf{p}_j+\hbar\mathbf{k}_{\mu}})t]+g^{*}_{\mu}S_{j,\mathbf{p}_j,\mathbf{k}_{\mu}}a^{\dagger}_{\mu}\exp[i(\Delta_{\mu}+\omega_{\mathbf{p}_j-\hbar\mathbf{k}_{\mu},\mathbf{p}_j})t]\} , \tag{25}$$

where

$$\omega_{\mathbf{p}\mathbf{p}'}=(\varepsilon_{\mathbf{p}}-\varepsilon_{\mathbf{p}'})/\hbar,\quad \varepsilon_{\mathbf{p}}=\mathbf{p}^2/2m , \tag{26}$$

and

$$S_{j,\mathbf{p}_j,\mathbf{k}}=|\mathbf{p}_1,\ldots,\mathbf{p}_j-\hbar\mathbf{k},\ldots,\mathbf{p}_N\rangle\times\langle 2_j;\mathbf{p}_1,\ldots,\mathbf{p}_j,\ldots,\mathbf{p}_N| . \tag{27}$$

By comparing the Hamiltonians (5) and (27), one is led to modify the computational rules (7) by replacing Δ_i with

$$\Delta_i'=\Delta_i\pm\omega_{\mathbf{p}_f,\mathbf{p}_{\mathrm{in}}} , \tag{28}$$

where + (−) corresponds to emission (absorption), and $\mathbf{p}_f$ and $\mathbf{p}_{\mathrm{in}}$ are the momenta following and prior to an atom-field interaction. Using the fact that $\mathbf{p}_f=\mathbf{p}_{\mathrm{in}}\mp\hbar\mathbf{k}_i$ [where the − (+) sign corresponds to absorption (emission)], one finds

$$\Delta_i'=\Delta_i-\mathbf{k}_i\cdot\mathbf{p}_{\mathrm{in}}/m\pm\omega_{\mathbf{k}_i} , \tag{29}$$

where

$$\omega_{\mathbf{k}}=\hbar\mathbf{k}^2/2m \tag{30}$$

is a recoil frequency. The difference between the right-hand side of (29) and (24) is of order $\omega_{\mathbf{k}}$ and can lead to RIR [3]. It is important to note that, once recoil effects are included, the law of conservation of probability for each momentum subclass of atoms no longer strictly

holds, i.e., $\rho_{11}(\mathbf{p})+\rho_{22}(\mathbf{p})\neq$const. As a result, resonances characterized by the inverse of the effective ground-state lifetime can appear in the 4WM line shapes [8].

In calculating the probability of 4WM emission, one must average over the initial state of the atomic ensemble. This procedure leads to an average over the velocity (or momentum) distribution of the particles. One might expect that the final result takes the form a probability integrated over a velocity distribution. It is seen below, however, that the final result is of the form of the square of a single-particle probability *amplitude* integrated over velocity. This is analogous to the density-matrix approach where the 4WM signal is proportional to the square of a velocity-integrated single-particle dipole density-matrix element.

Consider, for example, that part of the emission probability δP associated with $|C_{132\mathbf{k}}|^2$. In working with probability amplitudes in the momentum representation, one must calculate the probability amplitude $b(\mathbf{p}_1,\ldots,\mathbf{p}_j,\ldots,\mathbf{p}_N;n_1-1,n_2-1,n_3+1,1_{\mathbf{k}};t)$ for all atoms to be in state 1, having momenta $\mathbf{p}_1,\ldots,\mathbf{p}_j,\ldots,\mathbf{p}_N$, and for one photon to be absorbed from each of fields 1 and 2 and a photon emitted into each of fields 3 and $\mathbf{k}$. Using perturbation theory, it is easy to see that, corresponding to the amplitude $C_{132\mathbf{k}}$, one finds

$$b(\mathbf{p}_1,\ldots,\mathbf{p}_j,\ldots,\mathbf{p}_N;n_1-1,n_2-1,n_3+1,1_{\mathbf{k}};t) \propto \sum_j C_{132\mathbf{k}}(\mathbf{p}_j) \times b(\mathbf{p}_1,\ldots,\mathbf{p}_j-\hbar\bar{\mathbf{k}},\ldots,\mathbf{p}_N;n_1,n_2,n_3,0_{\mathbf{k}};0)\ ,$$

where $C_{132\mathbf{k}}(\mathbf{p})$ is the value of $C_{132\mathbf{k}}$ appropriately modified by the replacements (29) and $\bar{\mathbf{k}}$ is defined by (3). In forming probabilities, one arrives at a sum over j and j' involving products of the form

$$C_{132\mathbf{k}}(\mathbf{p}_j)C^*_{132\mathbf{k}}(\mathbf{p}_{j'}) \times b(\mathbf{p}_1,\ldots,\mathbf{p}_j-\hbar\bar{\mathbf{k}},\ldots,\mathbf{p}_N;n_1,n_2,n_3,0_{\mathbf{k}};0)\, b^*(\mathbf{p}_1,\ldots,\mathbf{p}_{j'}-\hbar\bar{\mathbf{k}},\ldots,\mathbf{p}_N;n_1,n_2,n_3,0_{\mathbf{k}};0)\ .$$

Assuming that the initial density matrix is diagonal in momentum space, one can have an N^2 contribution to the line shape only if $\bar{\mathbf{k}}=\mathbf{0}$, which is precisely the momentum conservation condition (1a) necessary for phase matching. If $\bar{\mathbf{k}}=\mathbf{0}$, the integration over center-of-mass momenta and over a small range $\Delta\mathbf{k}$ centered at $\mathbf{k}=\mathbf{k}_1-\mathbf{k}_3+\mathbf{k}_2(\bar{\mathbf{k}}=\mathbf{0})$ is easily carried out. One arrives at a phase-matched contribution δP associated with $|C_{132\mathbf{k}}|^2$ given by

$$\delta P=\sum_{\mathbf{k}} A_{\mathbf{k}}\left|\int d\mathbf{p}\, W(\mathbf{p})C_{132\mathbf{k}}(\mathbf{p})\right|^2, \tag{31}$$

where $W(\mathbf{p})$ is the reduced, single-particle atomic momentum distribution and $A_{\mathbf{k}}$ is defined by (11) [11]. When the amplitudes corresponding to the other diagrams in Fig. 7 are added in, one arrives at a probability for phase-matched emission given by

$$P=\sum_{\mathbf{k}} A_{\mathbf{k}}\left|\sum_{\sigma(\neq\mu)}\int d\mathbf{p}\, W(\mathbf{p})C(\mu,\sigma;\mathbf{p})\right|^2 \tag{32}$$

where

$$C(\mu,\sigma;\mathbf{p})=C^{\mathrm{st}}(\mu,\sigma;\mathbf{p})+C^{\mathrm{sp}}(\mu,\sigma;\mathbf{p}) \tag{33}$$

and $C^{\mathrm{st}}(\mu,\sigma;\mathbf{p})$ and $C^{\mathrm{sp}}(\mu,\sigma;\mathbf{p})$ are the values of $C^{\mathrm{st}}(\mu,\sigma)$ and $C^{\mathrm{sp}}(\mu,\sigma)$ appropriately modified by the replacements (29).

B. Secular approximation

One can observe RIR by monitoring the 4WM signal as a function of the detuning $\delta=\Delta_{31}$ between fields 1 and 3. The RIR width γ_r is determined by the relaxation rate of the field-induced ground-state atomic gratings. In this subsection, we make a secular approximation and assume that $|\Delta_i|\gg\Gamma,ku,\gamma_r$ $(i=1,2,3,\mathbf{k})$. The quantity $u=p_0/m$ is the most probable atomic speed while p_0 is the most probable atomic momentum.

Our goal is to calculate corrections to the 4WM amplitude resulting from the inclusion of atomic recoil. The exact cancellation of terms varying as Δ^{-2} no longer occurs when recoil is included. The signal consists of two parts. First, there is a "background" term, calculated in Sec. II, which varies as Δ^{-3} and does not exhibit any resonance structure near $\delta=0$. Second, there is the RIR contribution which varies as Δ^{-2} and *does* exhibit resonance structure centered at $\delta=0$. If

$$\eta=\omega_{\mathbf{k}}|\Delta|/(ku)^2 \tag{34}$$

is much greater than unity, the RIR contribution to the signal dominates the background term [3]. For the present discussion, we shall assume this condition to be satisfied. As has been pointed out previously, the inequality $\eta\gg1$ is generally satisfied for atoms cooled below the Doppler limit of laser cooling.

We need keep only terms varying as Δ^{-2} to find the leading contribution to the RIR signal. Both the spontaneous amplitude and the third summand in the formula (12c) do not contribute to this order. For the remaining contributions to the stimulated amplitude one can use an integral representation similar to (10) and, after the replacement (29), obtain

$$C_{\mu3\sigma\mathbf{k}}(\mathbf{p})=\chi_1\chi_3^*\chi_2 g_{\mathbf{k}}^* \int_0^t dt_1\exp[i(\Delta_{\mathbf{k}}+\omega_{\mathbf{p}+\hbar\bar{\mathbf{k}},\mathbf{p}+\hbar(\mathbf{k}_\sigma+\mathbf{k}_{\mu3})})t_1] \times\int_0^{t_1} dt_2\exp[-i(\Delta_\sigma-\omega_{\mathbf{p}+\hbar(\mathbf{k}_\sigma+\mathbf{k}_{\mu3}),\mathbf{p}+\hbar\mathbf{k}_{\mu3}})t_2-\gamma(t_1-t_2)] \times\int_0^{t_2} dt_3\exp[i(\Delta_3+\omega_{\mathbf{p}+\hbar\mathbf{k}_{\mu3},\mathbf{p}+\hbar\mathbf{k}_\mu})t_3] \times\int_0^{t_3} dt_4\exp[-i(\Delta_\mu-\omega_{\mathbf{p}+\hbar\mathbf{k}_\mu,\mathbf{p}})t_4-\gamma(t_3-t_4)]\ , \tag{35}$$

where

$$\mathbf{k}_{ij}=\mathbf{k}_i-\mathbf{k}_j \ . \tag{36}$$

Using the fact that $\bar{\mathbf{k}}=0$ [condition (1a)], to order Δ^{-2} one finds

$$C_{\mu 3\sigma\mathbf{k}}(\mathbf{p})=-B^* g_{\mathbf{k}}^* \varphi(\omega_{3\mu}) \ , \tag{37a}$$

where

$$B=\chi_1^*\chi_3\chi_2^*/\Delta_1\Delta_2 \ , \tag{37b}$$

$$\varphi(\omega)=\int_0^t dt_1 \exp[i(\tilde{\Delta}_{\mathbf{k}\sigma}-\omega)t_1] \times\int_0^{t_1} dt_2 \exp[i(\tilde{\Delta}_{3\mu}+\omega)t_2] \ , \tag{37c}$$

$$\tilde{\Delta}_{ij}=\Delta_{ij}-\mathbf{k}_{ij}\cdot\mathbf{p}/m \ , \tag{37d}$$

and

$$\omega_{ij}=\omega_{\mathbf{k}_{ij}} \ . \tag{37e}$$

The remaining contribution to the stimulated amplitude, $C_{\sigma\mathbf{k}}C_{3\mu}^*$, is evaluated in a similar fashion. Making use of the equality $\int_0^t dt_1\int_0^t dt_2=\int_0^t dt_1\int_0^{t_1} dt_2+\int_0^t dt_2\int_0^{t_2} dt_1$, one can obtain

$$C_{\sigma\mathbf{k}}(\mathbf{p})C_{3\mu}^*(\mathbf{p})=(\Delta_\mu/\Delta_3)[B^* g_{\mathbf{k}}^* \varphi(-\omega_{3\mu})-C_{\sigma\mathbf{k}\mu 3}(\mathbf{p})] \ . \tag{38}$$

Combining Eqs. (37) and (38) and assuming that $|\tilde{\Delta}_{3\mu}|\ll|\Delta_3|$, one finds the amplitude

$$C(\mu,\sigma,\mathbf{p})\approx C^{\mathrm{st}}(\mu,\sigma,\mathbf{p})=-B^* g_{\mathbf{k}}^*[\varphi(\omega_{3\mu})-\varphi(-\omega_{3\mu})] \ . \tag{39}$$

It is convenient to change variables to $t_2'=t_1-t_2$ in (37c). After changing the order of integration over t_1 and t_2' and substituting the result into (39), one finds

$$C(\mu,\sigma,\mathbf{p})=g_{\mathbf{k}}^*\int_0^t dt' R_\mu(\mathbf{p},t')\bar{\xi}(\bar{\Delta},t,t') \ , \tag{40a}$$

where

$$R_\mu(\mathbf{p},t)=2iB^*\exp(-i\tilde{\Delta}_{3\mu}t)\sin(\omega_{3\mu}t) \tag{40b}$$

and

$$\bar{\xi}(\Delta,t,t')=[\exp(i\Delta t)-\exp(i\Delta t')]/i\Delta \ . \tag{40c}$$

Equations (40) imply that the frequency of coherent emission is centered near the point $\bar{\Delta}=0$ in accordance with the law of energy conservation (1b). However, the probability distribution of the emitted photons is not determined by the function $|\xi(\bar{\Delta})|^2$, as it was for stationary atoms.

After substituting (40a) in (32) one finds

$$I=\dot{P}=\int_0^t dt'\int_0^t dt'' R(t')R^*(t'')\sum_{\mathbf{k}} A_{\mathbf{k}}|g_{\mathbf{k}}|^2\eta(\bar{\Delta}) \ , \tag{41a}$$

where

$$R(t)=\sum_{\mu=1}^{2}\int d\mathbf{p}\, W(\mathbf{p})R_\mu(\mathbf{p},t) \ , \tag{41b}$$

$$\eta(\Delta)=\frac{\partial}{\partial t}[\bar{\xi}(\Delta,t,t')\bar{\xi}^*(\Delta,t,t'')] \ , \tag{41c}$$

and the equality $\bar{\xi}(\Delta,t,t)=0$ was used. It follows from the definition (41c) that $\eta(\Delta)$ can be expressed as

$$\eta(\Delta)=2\pi\delta(\Delta) \tag{42}$$

for $t>t'$ and $t>t''$. Consequently,

$$I=I_0|S(t)|^2 \ , \tag{43a}$$

where

$$S(t)=\int_0^t dt' R^*(t') \tag{43b}$$

and I_0 is given by (23). Using Eqs. (43b), (41b) and (40b) one can obtain

$$S(t)=B\sqrt{\pi}\sum_{\mu=1}^{2}(|\mathbf{k}_{3\mu}u|)^{-1} \times\{I[(\Delta_{3\mu}+\omega_{3\mu})/(|\mathbf{k}_{3\mu}|u),\mathbf{k}_{3\mu}ut) -I[(\Delta_{3\mu}-\omega_{3\mu})/(|\mathbf{k}_{3\mu}|u),\mathbf{k}_{3\mu}ut)]\} \ , \tag{44}$$

where

$$I(z,\boldsymbol{\alpha})=\pi^{-1/2}\int_0^\alpha d\tau\int d\mathbf{p}\, W(\mathbf{p})\exp[i(z-p_\alpha/p_0)\tau] \ , \tag{45}$$

$p_\alpha=\mathbf{p}\cdot\boldsymbol{\alpha}/\alpha$, and τ is dimensionless. For a Maxwell distribution function

$$W(\mathbf{p})=(\pi^{1/2}p_0)^{-3}\exp[-(\mathbf{p}/p_0)^2] \ , \tag{46}$$

$I(z,\alpha)$ is expressed through the plasma dispersion function [12]

$$w(z)=\exp(-z^2)[1+2i\pi^{-1/2}\int_0^z d\tau\exp(\tau^2)] \ , \tag{47}$$

as

$$I(z,\boldsymbol{\alpha})=w(z)-\exp[iz\alpha-\alpha^2/4]w(z+i\alpha/2) \ . \tag{48}$$

The two contributions to the line shape (44) are centered at the points $\Delta_{3\mu}=\pm\omega_{3\mu}=\pm\hbar/|\mathbf{k}_{3\mu}|^2/2m$; in the absence of recoil these terms cancel one another. The width associated with each term is of order

$$\gamma_r\sim\max\{1/t,|\mathbf{k}_{3\mu}u|\} \ . \tag{49}$$

Assuming that $\omega_{\mathbf{k}}\ll\gamma_r$, one can expand (44) around $\omega_{3\mu}=0$ to obtain

$$S(t)=2B\sqrt{\pi}\sum_{\mu=1}^{2}[\omega_{3\mu}/(|\mathbf{k}_{3\mu}|u)^2] \times I'[\Delta_{3\mu}/(|\mathbf{k}_{3\mu}|u),\mathbf{k}_{3\mu}ut] \tag{50}$$

where

$$I'(z,\boldsymbol{\alpha})=\frac{\partial}{\partial z}I(z,\boldsymbol{\alpha}) \ . \tag{51}$$

For the Maxwellian distribution (46),

$$I'(z,\alpha)=2i\pi^{-1/2}[1-\exp(iz\alpha-\alpha^2/4)]-2zI(z,\alpha) . \quad (52)$$

If the background term is not negligible, one should add a term

$$S_{\rm bck}=-2iB[\Delta_3^{-1}+\Delta_{\mathbf{k}}^{-1}] \quad (53)$$

to Eq. (50) [13].

Let us consider a 4WM geometry in which fields 1 and 2 counterpropagate along the x axis and field 3 makes a small angle θ relative to field 1, i.e.,

$$\mathbf{k}_1=\underline{k}\hat{\mathbf{x}},\quad \mathbf{k}_2=-k\hat{\mathbf{x}},\quad \mathbf{k}_3=k_3(\hat{\mathbf{x}}+\theta\hat{\mathbf{y}})\approx k(\hat{\mathbf{x}}+\theta\hat{\mathbf{y}}) . \quad (54)$$

All incident fields, as well as the signal field, are polarized in the $\hat{\mathbf{z}}$ direction. For this geometry,

$$\omega_{31}=\omega_{\mathbf{k}}\theta^2 \quad (55a)$$

and

$$\omega_{32}=4\omega_{\mathbf{k}} . \quad (55b)$$

An interpretation of the recoil-induced line in terms of the Raman transitions between states differing in center-of-mass energy has been given previously [3]. There are essentially two types of resonances. The first involves the formation of atomic gratings by fields 1 and 3. The width of the corresponding RIR is $\max(ku\theta,t^{-1})$. We refer to this contribution as the "forward" Raman line. The second term involves the formation of atomic gratings by fields 2 and 3, leading to a RIR having width $\max(2ku,t^{-1})$. We refer to this contribution as a "backward" Raman line. There are additional contributions to the line shape from gratings formed by fields 2 and $\mathbf{k}$ and fields 1 and $\mathbf{k}$. Owing to the momentum conservation condition (1a), the 2-$\mathbf{k}$ grating corresponds to a forward Raman contribution and the 1-$\mathbf{k}$ grating to a backward Raman contribution.

For $\theta\ll 1$, three different regimes should be considered:

$$t\ll 1/ku , \quad (56a)$$

$$1/ku\ll t\ll 1/ku\theta . \quad (56b)$$

$$t\gg 1/ku\theta , \quad (56c)$$

when the time of interaction is short enough to broaden both the forward and backward Raman lines, when it is small enough to broaden only the forward Raman line, and when it is sufficiently large so as not to affect the forward or backward line width.

$t\ll 1/(ku)$. In this limit all Doppler dephasing can be neglected. In the expression

$$S(t)=2B\sqrt{\pi}\sum_{\mu=1}^{2}[\omega_{3\mu}/(|\mathbf{k}_{3\mu}|u)^2] \times I'[\Delta_{3\mu}/(|\mathbf{k}_{3\mu}|u),\mathbf{k}_{3\mu}ut] \quad (57)$$

one can substitute

$$I(z,\alpha)\approx\pi^{-1/2}[\exp(iz\alpha)-1]/iz . \quad (58)$$

Both Raman lines have the same widths, but the relative intensities of the forward to backward amplitudes is

$$\omega_{31}/\omega_{32}\sim\theta^2\ll 1 , \quad (59)$$

enabling one to neglect the forward Raman component. The 4WM signal is

$$I=I_0|4B\omega_{\mathbf{k}}|^2t^4F(\delta t) , \quad (60a)$$

where

$$F(x)=|f(x)|^2 \quad (60b)$$

and

$$f(x)=2[(1-ix)e^{ix}-1]/x^2 . \quad (60c)$$

Thus both the amplitude and width are functions of t and Fermi's golden rule is not strictly applicable in this limit. On the other hand, it follows from Eqs. (43a), (23), and (11) that one can write I as $I=2\pi\sum_{\mathbf{k}}|g_{\mathbf{k}}S(t)|^2A_{\mathbf{k}}\delta(\bar{\Delta})$, which has the form of Fermi's golden rule with a time-dependent matrix element $g_{\mathbf{k}}S(t)$. For $kut\ll 1$, one can deduce from Eq. (51) that $S(t)\propto\omega_{\mathbf{k}}t^2f(\Delta_{31}t)$. This ex-

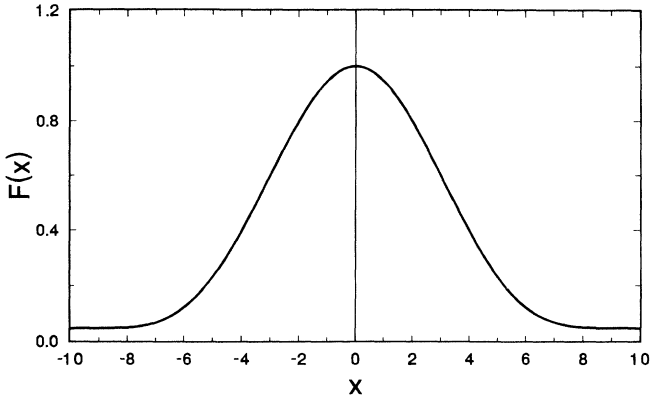

FIG. 8. Recoil-induced universal line-shape function $F(x)$ for short interaction times, $t\ll(ku)^{-1}$. The abscissa is in dimensionless units $x=\delta t$.

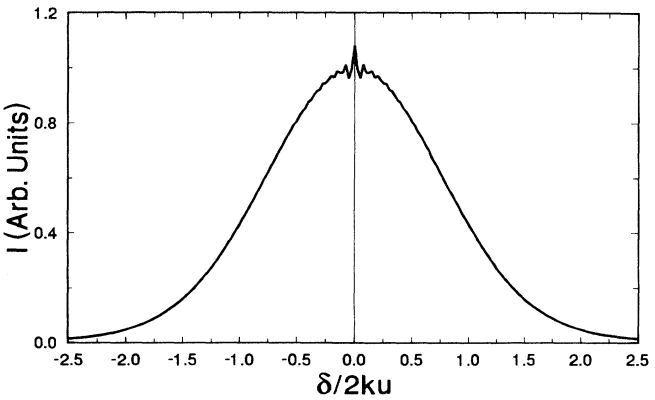

FIG. 9. Recoil-induced line shape I as a function of $\delta/2ku$ in the limit $(ku)^{-1}\ll t\ll(ku\theta)^{-1}$. The parameters chosen for this plot are $\theta=0.008$ and $kut=50$. Both the forward and backward Raman components are visible.

plains the t^4 dependence of the line shape.

The result (60) is universal. It describes the coherent emission of the medium for short interaction times, independent of the atomic distribution function and the relaxation processes on the lower level. A plot of $F(x)$ is shown in Fig. 8. For small and large x, one has

$$F(x)=\begin{cases}[1-(x^2/18)], & |x|\ll 1\\ 4/x^2, & |x|\gg 1\end{cases}. \tag{61}$$

$(1/ku)\ll t\ll 1/(ku\theta)$. In this limit one can set $\alpha=\infty$ for the backward Raman line and $p_\alpha=0$ for the forward line in Eq. (45) for $I(z,\alpha)$. Using this result in Eq. (50), one finds

$$S(t)=B\omega_{\mathbf{k}}\{i\theta^2t^2f(\Delta_{31}t) +4(ku)^{-2}[i-\pi^{1/2}z_2w(z_2)]\}, \tag{62a}$$

where

$$z_\mu=\Delta_{3\mu}/(k_{3\mu}u). \tag{62b}$$

The ratio of the forward to backward amplitude is $(kut\theta)^2\ll 1$, and the ratio of the forward to backward resonance width is $(kut)^{-1}\ll 1$. The forward Raman contribution to $S(t)$ is $\omega_{31}t^2f(\Delta_{31}t)$ as it was for the $t\ll(ku)^{-1}$ case, while the backward Raman contribution is proportional to $\omega_{\mathbf{k}}/(ku)^2$. In analogy with the forward Raman line, the backward Raman contribution can be interpreted as being proportional to $\omega_{32}t_{\rm coh}^2f(\Delta_{31}t_{\rm coh})=4\omega_{\mathbf{k}}t_{\rm coh}^2f(\Delta_{31}t_{\rm coh})$, where the effective coherence time $t_{\rm coh}\approx(2ku)^{-1}$ in the large Doppler broadening limit. The line shape is plotted in Fig. 9. Recall that $\Delta_{31}\equiv\delta$.

$t>>1/(ku\theta)$. In this limit Doppler broadening dominates both the forward and backward Raman lines and one finds

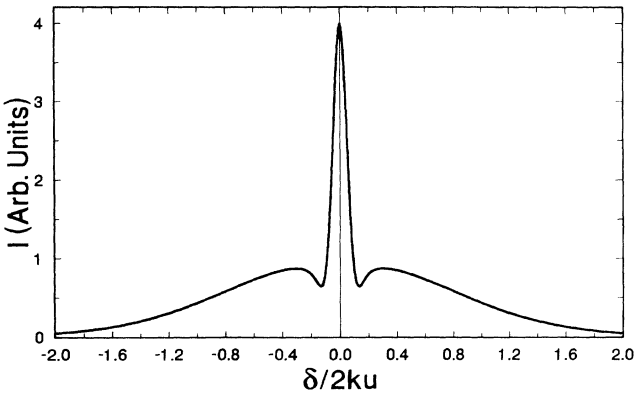

FIG. 10. Recoil-induced line shape I as a function of $\delta/2ku$ in the limit $t>>(ku\theta)^{-1}$, with $\theta=0.15$. The forward and backward Raman components have the same amplitudes in this limit.

$$S=4B\omega_{\mathbf{k}}(ku)^{-2}\{2i-\pi^{1/2}[z_1\omega(z_1)+z_2w(z_2)]\}, \tag{63}$$

Expression (63) coincides with formula, derived in Ref. [3], when that formula is evaluated in the secular approximation. The line shape is plotted in Fig. 10. Note the constructive interference between he forward and backward contributions near $\delta=0$.

C. Arbitrary detunings

For arbitrary ratios of Δ_i/Γ, the 4WM line shape is derived in Appendix B to lowest order in the parameter $(\gamma t)^{-1}\ll 1$. From formula (B24) one has

$$I=I_0|S(t)|^2, \tag{64a}$$

$$S(t)=\sum_{\sigma(\neq\mu)}[S_{\mu\sigma}(t)-S^0_{\mu\sigma}(t)], \tag{64b}$$

$$\begin{aligned}S_{\mu\sigma}(t)=\chi_1^*\chi_3\chi_2^*\int d\mathbf{p}\,\mathbf{W}(\mathbf{p})\int_0^t dt'\Bigg[&\exp[i(\tilde\Delta_{3\mu}+\omega_{3\mu})t']\\ &\times\left\{[\gamma+i(\tilde\Delta_\mu-\omega_{\mathbf{k}})]\left[\gamma+i\left[\tilde\Delta_\sigma-\omega_{\mathbf{k}}+\frac{\hbar}{m}\mathbf{k}_\sigma\cdot\mathbf{k}_{3\mu}\right]\right]\right\}^{-1}\\ &+\exp[i(\tilde\Delta_{3\mu}-\omega_{3\mu})t']\{[\gamma+i(\tilde\Delta_\sigma-\omega_{\mathbf{k}})][\gamma-i(\tilde\Delta_3-\omega_{\mathbf{k}})]\}^{-1}\\ &-\Gamma\{[\gamma+i(\tilde\Delta_\mu-\omega_{\mathbf{k}})][\gamma-i(\tilde\Delta_3-\omega_{\mathbf{k}})]\}^{-1}\\ &\times\int d\mathbf{n}_{\mathbf{q}}N_{\mathbf{q}}\exp\left[i\left[\tilde\Delta_{3\mu}+\frac{\hbar}{m}\mathbf{q}\cdot\mathbf{k}_{3\mu}\right]t'\right]\left[\gamma+i\left[\tilde\Delta_\sigma-\omega_{\mathbf{k}}-\frac{\hbar}{m}\mathbf{k}_\sigma\cdot(\mathbf{k}_\mu-\mathbf{q})\right]\right]^{-1}\Bigg],\end{aligned} \tag{64c}$$

where

$$N_{\mathbf{q}}=|g_{\mathbf{q}}|^2\Big/\int d\mathbf{n}_{\mathbf{q}}|g_{\mathbf{q}}|^2, \tag{64d}$$

$$S^0_{\mu\sigma}(t)=S_{\mu\sigma}(t)\Big|_{\hbar\to 0}, \tag{64e}$$

and $\mathbf{n}_{\mathbf{q}}=\mathbf{q}/q$. We have set $\omega_{\mathbf{k}_i}=\omega_{\mathbf{k}}$ in these equations. To be specific we choose states 1 and 2 to be the $m=0$

sublevels of angular momentum states $J_1=0$ and $J_2=1$, respectively. In that case

$$N_{\mathbf{q}}=(3/8\pi)\sin^2\theta_{\mathbf{q}} , \tag{65}$$

where $\theta_{\mathbf{q}}$ is the angle between vectors $\mathbf{q}$ and $\hat{\mathbf{z}}$.

One finds a new RIR component centered at $\Delta_{3\mu}=-\hbar\bar{\mathbf{q}}\cdot\mathbf{k}_{3\mu}=0$ in addition to those centered at $\Delta_{3\mu}=\pm\omega_{3\mu}$. The origin of this new resonance can be traced to terms involving spontaneous emission. It is possible to resolve the resonances centered at $\Delta_{3\mu}=0,\pm\omega_{3\mu}$, if $\omega_{\mathbf{k}}>\gamma_r$; however, in most experimental situations we encounter the opposite limit

$$\omega_{\mathbf{k}}\ll\gamma_r , \tag{66}$$

which is adopted in this work. For the remainder of the discussion, it is furthermore assumed that

$$\gamma\gg ku , \tag{67}$$

a limit valid for atoms cooled to or below the Doppler limit of laser cooling.

When inequality (67) is satisfied, one can replace the $\tilde{\Delta}_i$ in Eq. (64c) by Δ_i and carry out the momentum integration to obtain

$$\begin{aligned}S_{\mu\sigma}(t)=&\chi_1^*\chi_3\chi_2^*[\pi^{1/2}/(|\mathbf{k}_{3\mu}|u)]\\&\times\left\{I[(\Delta_{3\mu}+\omega_{3\mu})/(|\mathbf{k}_{3\mu}|u),\mathbf{k}_{3\mu}ut]\left\{[\gamma+i(\Delta_\mu-\omega_{\mathbf{k}})]\left[\gamma+i\left[\Delta_\sigma-\omega_{\mathbf{k}}+\frac{\hbar}{m}\mathbf{k}_\sigma\cdot\mathbf{k}_{3\mu}\right]\right]\right\}^{-1}\right.\\&+I[(\Delta_{3\mu}-\omega_{3\mu})/(|\mathbf{k}_{3\mu}|u),\mathbf{k}_{3\mu}ut]\{[\gamma+i(\Delta_\sigma-\omega_{\mathbf{k}})][\gamma-i(\Delta_3-\omega_{\mathbf{k}})]\}^{-1}\\&-\Gamma\{[\gamma+i(\Delta_\mu-\omega_{\mathbf{k}})][\gamma-i(\Delta_3-\omega_{\mathbf{k}})]\}^{-1}\int d\mathbf{n}_{\mathbf{q}}N_{\mathbf{q}}I\left[\left[\Delta_{3\mu}+\frac{\hbar}{m}\mathbf{q}\cdot\mathbf{k}_{3\mu}\right]\Big/(|\mathbf{k}_{3\mu}|u),\mathbf{k}_{3\mu}ut\right]\\&\left.\times\left[\gamma+i\left[\Delta_\sigma-\omega_{\mathbf{k}}-\frac{\hbar}{m}\mathbf{k}_\sigma\cdot(\mathbf{k}_\mu-\mathbf{q})\right]\right]^{-1}\right\} .\end{aligned} \tag{68}$$

Since $\omega_{\mathbf{k}}$ is smaller than all other relevant frequency parameters, one can expand the energy denominators and I functions about $\omega_{\mathbf{k}}=0$. In that case the parameters

$$\beta_1=\omega_{\mathbf{k}}/\gamma_r , \tag{69a}$$

$$\beta_2=\omega_{3\mu}/\gamma_r=\omega_{\mathbf{k}}(\theta^2\delta_{\mu1}+4\delta_{\mu2})/\gamma_r , \tag{69b}$$

$$\beta_3=\omega_{\mathbf{k}}\omega_{3\mu}/\gamma_r^2=\omega_{\mathbf{k}}^2(\theta^2\delta_{\mu1}+4\delta_{\mu2})/\gamma_r^2 \tag{69c}$$

determine the weights of the various contributions to the RIR line shape. For the backward Raman line ($\mu=2$), the parameter β_2 dominates. For the forward Raman line ($\mu=1$) all contributions can be of the same order. Expanding Eq. (68) to lowest order in β_i and keeping only the term proportional to β_2 for $\mu=2$, one finds

$$\begin{aligned}S_{\mu\sigma}(t)=&-i2\pi^{1/2}\chi_1^*\chi_3\chi_2^*\omega_{3\mu}(|\mathbf{k}_{3\mu}|u)^{-2}\Delta_\mu[(\gamma+i\Delta_\sigma)(\gamma^2+\Delta_\mu^2)]^{-1}\\&\times\{I'[\Delta_{3\mu}/(|\mathbf{k}_{3\mu}|u),\mathbf{k}_{3\mu}ut)-2\delta_{\mu1}(ku\gamma/\Delta_1\theta)[(\gamma+i\Delta_2)^{-1}I[\Delta_{3\mu}/(|\mathbf{k}_{3\mu}|u),\mathbf{k}_{3\mu}ut)\\&+\tfrac{2}{5}i\omega_{\mathbf{k}}(ku)^{-2}I''[\Delta_{3\mu}/(|\mathbf{k}_{3\mu}|u],\mathbf{k}_{3\mu}ut)]\} ,\end{aligned} \tag{70}$$

where the inequality $|\Delta_{3\mu}|\ll|\Delta_3|\sim\gamma$ was used. Together with Eqs. (64a) and (64b), Eq. (70) determines the line shape in the limit case $\gamma\gg ku$. If the background term is not negligible compared with the RIR amplitude, one should add a term

$$S_{bck}=\chi_1^*\chi_3\chi_2^*[\Gamma+i(\Delta_1+\Delta_2)][(\gamma^2+\Delta_\mu^2)(\gamma+i\Delta_\sigma)^2]^{-1} \tag{71}$$

to Eq. (70) [13].

In the preceding section, it was assumed that $\Delta_1=\Delta_2$. In order to spectrally separate the backward and forward Raman lines, it is advantageous to choose different pump frequencies such that

$$|\Delta_{12}|\gg\gamma_r . \tag{72}$$

Consequently, one can consider independently the forward and backward Raman components of the RIR in analogy with other Raman-like responses [14]. The quantity $S(t)$ takes on the limiting forms

$$S(t)=4i\pi^{1/2}\chi_1^*\chi_3\chi_2^*(\omega_{\mathbf{k}}/ku\theta)[(\gamma+i\Delta_2)(\gamma^2+\Delta_1^2)]^{-1}$$
$$\times\{[\gamma/(\gamma+i\Delta_2)]I(\Delta_{31}/ku\theta,\mathbf{k}_{31}ut)-(\Delta_1\theta/2ku)I'[(\Delta_{31}/ku\theta),\mathbf{k}_{31}ut]$$
$$+\tfrac{2}{5}i[\gamma\omega_{\mathbf{k}}/(ku)^2]I''[(\Delta_{31}/ku\theta),\mathbf{k}_{31}ut]\}\ , \tag{73a}$$
$$S(t)=-2i\pi^{1/2}\chi_1^*\chi_3\chi_2^*\omega_{\mathbf{k}}(ku)^{-2}\Delta_2[(\gamma+i\Delta_1)(\gamma^2+\Delta_2^2)]^{-1}I'[(\Delta_{32}/2ku),\mathbf{k}_{32}ut] \tag{73b}$$

for the forward and backward Raman contributions, respectively.

Finally, we consider 4WM for exactly parallel pump and probe fields. If $\theta=0$, all Doppler dephasings for the forward Raman line vanish. There is still a forward Raman resonance centered at $\Delta_{31}=0$, although the physical origin of the resonance differs from that for the $\theta\neq0$ limit [3]. From Eq. (73a), one finds the RIR amplitude

$$S(t)=4i\chi_1^*\chi_3\chi_2^*\gamma[(\gamma^2+\Delta_1^2)(\gamma+i\Delta_2)^2]^{-1}$$
$$\times\omega_{\mathbf{k}}t\{[\exp(i\Delta_{31}t)-1]/(i\Delta_{31}t)\}\ . \tag{74}$$

Comparing this formula and Eq. (71) one concludes that, for $\theta=0$, the RIR contribution is greater than the background contribution provided

$$t\gtrsim\omega_{\mathbf{k}}^{-1}\{1+[(\Delta_1+\Delta_2)/\Gamma]^2\}^{1/2}\ . \tag{75}$$

Since $\omega_{\mathbf{k}}$ is typically of order $10^4\ \mathrm{s}^{-1}$, interaction times $t\gtrsim100\ \mu\mathrm{s}$ are needed to observe the RIR resonances with $\theta=0$ [15].

It is interesting to note that if the background is comparable to the RIR signal, the 4WM line shape can differ qualitatively for $ku\theta t\gg1$ and $\theta=0$, for an appropriate choice of Δ_1 and Δ_2 [$|\Delta_i|\gg\gamma$, $|\Delta_1+\Delta_2|\gg\Gamma$, and $(\Delta_1+\Delta_2)<0$, $\Delta_1>0$, $\Delta_2<0$, or $(\Delta_1+\Delta_2)>0$, $\Delta_1<0$, $\Delta_2>0$]. The line shapes in these limits [with the background contribution (71) added to Eqs. (73a) and (74)] are shown in Fig. 11. One sees that the RIR appears as a peak (dip) on the background for the $\theta=0$ ($ku\theta t\gg1$) case. If $\Delta_1=\Delta_2$ the background and backward Raman signals are superimposed on the forward signal. In this limit both the $ku\theta t\gg1$ and $\theta=0$ signals appear as peaks, in contrast to the situation in pump-probe spectroscopy where the sign of the dispersion shape differs for $\theta=0$ and $ku\theta t\gg1$ [3].

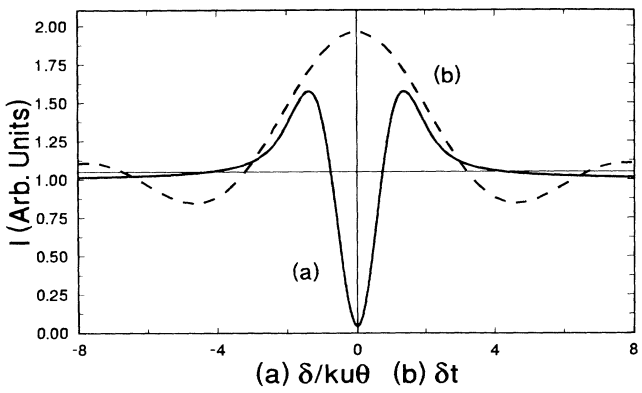

FIG. 11. Plots of (a) the forward Raman line [square of Eq. (73a) plus Eq. (71)] as a function of $\delta/ku\theta$ in the limit $ku\theta t\gg1$ and (b) the line shape for $\theta=0$ [square of Eq. (74) plus Eq. (71)], assuming the background contribution [Eq. (71) of the text] is comparable to the recoil-induced signal. Detuning $\delta=\Delta_{31}$. The parameters chosen for these plots are $A=2\omega_{\mathbf{k}}\Delta_1\Delta_2/[k^2u^2(\Delta_1+\Delta_2)]=-0.8$ and $B=2\gamma\omega_{\mathbf{k}}t/(\Delta_1+\Delta_2)=0.4$. Had we taken $A>0$ and $B<0$, the peak and dip would be reversed The graphs are normalized to a background intensity of unity.

IV. DISCUSSION

The signal for nearly degenerate four-wave mixing (4WM) has been calculated using an amplitude approach. No fewer than 14 distinct amplitudes, each corresponding to a different final state, contribute to the signal. When these amplitudes are squared and summed, however, they can be regrouped into a form in which the signal is expressed as the square of the sum of five terms. With the final result expressed in this form, the calculation using the amplitude approach is not much more complicated, and may even be easier, than the corresponding calculation using a density-matrix approach. Moreover, one gains additional insight into the origin of the signal using an amplitude approach.

One is interested in studying the intensity of the 4WM line shape as a function of the detuning δ between the "probe" and "pump" fields (in this work fields 1 and 2 are pump fields and field 3 is a probe field). With the neglect of recoil and collisional effects, the 4WM line shape contains no resonance structure centered at $\delta=0$. In the secular approximation, it is tempting to try to explain the 4WM line shape as arising solely from the amplitude shown in Fig. 7(a), in which two pump photons are absorbed and a probe and signal photon emitted. The absence of the $\delta=0$ resonance is then explained as an interference effect between the two "time orderings" (i.e, field 1 absorbed, 3 emitted, 2 absorbed, $\mathbf{k}$ emitted or field 2 absorbed, $\mathbf{k}$ emitted, 1 absorbed, 3 emitted) that contribute to this amplitude. In a large part, this interference *is* responsible for the disappearance of the $\delta=0$ resonance but it is not the whole story. If one kept only the

amplitude corresponding to Fig. 7(a), the resulting 4WM signal would contain terms that are manifestly incorrect. It is necessary to include the contributions from all the remaining diagrams to consistently explain the 4WM line shape. Amplitudes involving final states in which some of the atoms are excited as well as amplitudes involving photons emitted into radiation field modes other than the phase-matched mode $\mathbf{k}$ contribute.

When effects related to atomic recoil are included, a resonance structure centered at $\delta=0$ appears. In the secular approximation, the emergence of the $\delta=0$ resonance can be linked to the fact that there is a phase-matched contribution from the two components of Fig. 7(a) that no longer cancel to order Δ^{-2} when recoil is included. In some sense, this explanation is consistent with the idea of "the destruction of destructive interference" [4]. Two additional features emerged from the calculation. First, the way in which the line shape, which is the velocity average of a squared amplitude, could be expressed as the square of a velocity-averaged amplitude followed naturally from this approach. Second, it was seen that the results, obtained for a finite atom-field interaction time, can differ from the corresponding results obtained assuming an effective ground-state lifetime. The results differ whenever the interaction time is not the longest time scale in the problem, as is the case for parallel pump and probe fields ($\theta=0$) in which $(ku\theta)^{-1}\sim\infty>t$. For $\theta=0$, both stimulated and spontaneous terms contribute to the recoil-induced resonance. The physical origin of this term has been explained previously [3] and is related to slight differences in the one- and three-photon resonance denominators resulting from atomic recoil. It should be noted that the amplitude calculation is actually simpler than the corresponding density-matrix calculation in the finite interaction time model.

The amplitude calculation of the collision-induced resonances given in Appendix B is undoubtedly much more complicated than the corresponding calculation using a density-matrix approach. However, it is evident using the amplitude approach that the collision-induced resonances can be linked to amplitudes involving the emission of spontaneous photons into modes other than the phase-matched mode $\mathbf{k}$. In other words, the collision-induced resonances *cannot* be interpreted as arising from a process in which two pump photons are absorbed and a probe and signal photon emitted. This result is similar to that obtained in a model problem involving three-wave mixing [2], but the situation is somewhat more complicated here. In contrast to the three-wave mixing case, there is considerable cancellation between the stimulated and spontaneous amplitudes in the present calculation.

The calculation can be extended to "open" systems by adding an additional level (state 3) to which state 2 can decay, but which, itself, is not affected by the external fields. One must then add contributions, similar to those in Figs. 7(g)–7(j) involving spontaneous photons which leave the atoms in state 3. There is an important difference, however. Only diagrams in which the spontaneous photon is the *last* to enter contribute since any decay to state 3 at an earlier stage would decouple the atoms from the field. As a result there is no longer a destructive interference effect between different "time-ordered" diagrams. Consequently, a narrow resonance centered at $\delta=0$ appears [16] whose width is determined by the inverse of the atom-field interaction time.

We have seen that the amplitude approach can provide physical insight into the underlying physical mechanisms involved in nonlinear spectroscopy. Recently, this approach has been used to analyze the probe absorption spectrum in the presence of a pump field that is detuned from the probe by an amount δ [17]. It is found that the resonance structure centered at $\delta=0$ that appears to second order in the pump intensity can be explained in terms of amplitudes involving the emission of two spontaneous photons. A similar "field-induced resonance" [18] would also appear in 4WM if our calculation is extended to the next order in the pump field intensity.

ACKNOWLEDGMENTS

We should like to thank J. Guo for helpful discussions. This work is supported by the U. S. Office of Naval Research, by the National Science Foundation through Grants Nos. PHY-9113590 and INT-8815306, and by a New York University Research Challenge Fund Grant.

APPENDIX A: AMPLITUDE DIAGRAMS

It turns out that 14 distinct amplitudes contribute to the probability for 4WM in the phase-matched direction $\mathbf{k}=\mathbf{k}_1-\mathbf{k}_3+\mathbf{k}_2$. These amplitudes are represented schematically in the ten components (a)–(j) of Fig. 7. In Fig. 7, *as well as in the entire discussion of this appendix,* the indices μ, σ, λ, and ν can take on the values 1 or 2, with $\mu\neq\sigma,\lambda\neq\nu$. As such each of Figs. 7(b), 7(c), 7(f) (with $\mu=1,\sigma=2$ and $\mu=2,\sigma=1$) and 7(i) (with $\lambda=1,\nu=2$ and $\lambda=2,\nu=1$) represents two distinct amplitudes for a total 14 amplitudes. In this appendix, we outline a method for identifying these contributions.

Consider the first the stimulated amplitude. The number of photons in each incident field can increase by one, decrease by one, or remain unchanged. Thus, in principle, there are $3^3=27$ possible contributions to the stimulated amplitude. Since there is always a signal photon $\mathbf{k}$ emitted, the situation in which the photon number in all three fields remains unchanged must be ruled out. Moreover, since the phase-matched amplitude varies as $\exp[i(\mathbf{k}_1-\mathbf{k}_3+\mathbf{k}_2-\mathbf{k})\cdot\mathbf{r}]$, and since each up (down) arrow j leads to a factor $\exp(i\mathbf{k}_j\cdot\mathbf{r})[\exp(-i\mathbf{k}_j\cdot\mathbf{r})]$, one must always have an up μ (or σ) immediately preceding a down $\mathbf{k}$ arrow. The remaining arrows must be chosen in a manner consistent with phase matching for the chosen signal direction $\mathbf{k}$.

The simplest diagram one can imagine satisfying these conditions is shown in Fig. 7(a) and has been described in the text. The μ and σ arrows must be up and the 3 arrow down to satisfy the phase-matching condition. To get the remaining stimulated diagrams, one can "cut" the diagrams in Fig. 7(a) at any point other than between an up arrow σ (or μ) and the down arrow $\mathbf{k}$. The cut section containing the $\mathbf{k}$ arrow then serves as a building block for the remaining diagrams.

For example, if the first diagram of Fig. 7(a) is cut in the center, one obtains a building block having an up σ arrow and down $\mathbf{k}$ arrow. One multiplies this partial amplitude acting at atomic site j by a partial amplitude consisting of an up 3 arrow and down μ arrow acting at atomic site j' [see Fig. 7(b)]. When this amplitude is summed over j and j' and squared, one arrives at a phase-matched contribution to the signal, varying as N^2. It is also possible to let this cut partial amplitude stand alone, corresponding to a probability amplitude for the absorption of a σ photon and emission of a $\mathbf{k}$ photon, with all atoms in their ground states. This partial amplitude alone does not lead to phase-matched emission; however, when one adds to it the second set of diagrams in Fig. 7(c) representing the same final state and squares the total amplitude, the cross terms correspond to phase-matched emission in the desired direction. The remaining stimulated amplitude diagrams are obtained by cutting the diagrams of Fig. 7(a) such that the "building block" contains an up σ arrow, a down $\mathbf{k}$ arrow, and an up μ arrow, and following a procedure similar to that outlined above.

The spontaneous terms can be calculated in the same manner. At most two spontaneous photons $\mathbf{q}$ and $\mathbf{q}'$ can be emitted to this order in perturbation theory. Thus it is possible to have a photon absorbed from each of fields 1, 2, and 3, with the emission of photons $\mathbf{q}$, $\mathbf{q}'$, and $\mathbf{k}$ with all atoms in their ground states. It is impossible to have all photons absorbed at the same atomic site since this would lead to the incorrect phase factor $\exp[i(\mathbf{k}_1+\mathbf{k}_2+\mathbf{k}_3-\mathbf{k}-\mathbf{q}-\mathbf{q}')\cdot\mathbf{r}]$ One must have the fields absorbed at different atomic sites as shown in Fig. 7(g). The square of this amplitude will lead to phase-matched emission in the direction $\mathbf{k}=\mathbf{k}_1-\mathbf{k}_3+\mathbf{k}_2$. By cutting this diagram as described above, one arrives at the remaining diagrams in Fig. 7.

Table I lists the various probability amplitudes represented schematically in Fig. 7. The letters (a)–(j) correspond to the corresponding letters in Fig. 7. A "+" indicates emission into a field mode, a "−" indicates absorption, and a "0" indicates no change in photon number. Note that lines (b), (c), (f), and (i) actually correspond to two amplitudes each since (μ,σ) can take on two sets of values, (1,2) and (2,1). The remaining lines are unchanged under the exchange $\mu\leftrightarrow\sigma$, and correspond to a single amplitude, giving a total of 14 distinct amplitudes that contribute to the signal. The last column, labeled A, indicates the number of atoms excited in each process.

TABLE I. The letters (a)–(j) correspond to the diagrams of Fig. 7. A "+" corresponds to emission, a "−" to absorption, and a "0" to no change in photon number. The last column indicates the number of atoms excited in the process.

	σ	μ	3	$\mathbf{k}$	$\mathbf{q}$	$\mathbf{q}'$	A
(a)	−	−	+	+	0	0	0
(b)	−	+	−	+	0	0	0
(c)	−	0	0	+	0	0	0
(d)	−	−	−	+	0	0	2
(e)	−	−	0	+	0	0	1
(f)	−	0	−	+	0	0	1
(g)	−	−	−	+	+	+	0
(h)	−	−	0	+	+	0	0
(i)	0	−	−	+	+	0	0
(j)	−	−	−	+	+	0	1

APPENDIX B: BEYOND THE SECULAR APPROXIMATION WITH THE INCLUSION OF COLLISIONAL EFFECTS

In this appendix we extend the results of the text to allow for arbitrary ratios of detunings Δ_i to upper state decay rate $\Gamma=2\gamma$. It is assumed that

$$(\gamma t)^{-1}\ll 1 \tag{B1}$$

and all results are calculated to lowest nonvanishing order in this parameter. In subsection 1, the results of Sec. II for the background term are generalized. Collisional effects are included in subsection 2, in which the collision-induced resonances are discussed. In subsection 3, the results of Sec. III for the recoil-induced resonances are generalized.

1. Case of purely radiative broadening

The calculation of the various C parameters needed in Eqs. (12) are easily performed using the rules (7). Equations (14) for the amplitudes are replaced by

$$C_3=-i[\chi_3/(\gamma-i\Delta_3)]\exp(-i\Delta_3 t)\ , \tag{B2a}$$

$$C_{31}=-[\chi_3\chi_1^*/(\gamma-i\Delta_3)][\xi(\Delta_{13})-(\gamma-i\Delta_1)^{-1}]\ ,$$

$$C_{1\mathbf{k}2}=i\chi_1 g_{\mathbf{k}}^*\chi_2[(\gamma-i\Delta_1)(\gamma-i\Delta_2)]^{-1}\times\exp(-i\Delta_2 t)\xi(\Delta_{\mathbf{k}1})\ , \tag{B2c}$$

$$C_{132\mathbf{k}}=\chi_1\chi_3^*\chi_2 g_{\mathbf{k}}^*[(\gamma-i\Delta_1)(\gamma-i\Delta_2)]^{-1}\times\{\xi(\Delta_{\mathbf{k}2},\Delta_{31})-[\gamma-i(\Delta_1+\Delta_2-\Delta_3)]^{-1}\xi(\bar{\Delta})-(\gamma-i\Delta_3)^{-1}\xi(\Delta_{\mathbf{k}2})\}\ . \tag{B2d}$$

Other members in the expression for the stimulated amplitude can be found from Eqs. (B2) using permutations of the indices. From Eqs. (12c) and (B2), one can obtain

$$C^{\mathrm{st}}(\mu,\sigma)=\chi_1\chi_3^*\chi_2 g_{\mathbf{k}}^*[(\gamma-i\Delta_1)(\gamma-i\Delta_2)(\gamma+i\Delta_3)]^{-1}\times\{\Gamma\xi(\Delta_{3\mu})\xi(\Delta_{\mathbf{k}\sigma})-\xi(\bar{\Delta})(\gamma+i\Delta_3)[(\gamma-i(\Delta_1+\Delta_2-\Delta_3))^{-1}+(\gamma-i(\Delta_1+\Delta_2-\Delta_{\mathbf{k}}))^{-1}]-\xi(\Delta_{\mathbf{k}\sigma})[1+(\gamma+i\Delta_3)/(\gamma-i\Delta_3)+(\gamma-i\Delta_\mu)/(\gamma+i\Delta_\mu)]-\xi(\Delta_{3\mu})(\Gamma+i\Delta_{3\mu})/(\gamma-i\Delta_{\mathbf{k}})\}\ . \tag{B3}$$

To calculate the spontaneous amplitude (12d) one can use Eqs. (B2) with appropriate indices to arrive at

$$C^{\rm sp}(\mu,\sigma)=-\chi_1\chi_3^*\chi_2 g_{\mathbf{k}}^*[(\gamma-i\Delta_1)(\gamma-i\Delta_2)(\gamma+i\Delta_3)]^{-1}$$
$$\times\sum_{\mathbf{q}}|g_{\mathbf{q}}|^2\{\xi(\Delta_{3q})-(\gamma+i\Delta_{\mathbf{q}})^{-1}\}(\xi(\Delta_{\mathbf{k}\sigma})\xi(\Delta_{\mathbf{q}\mu})-\xi(\Delta_{\mathbf{k}\sigma}+\Delta_{\mathbf{q}\mu})\{[\gamma-i(\Delta_\sigma+\Delta_{\mu\mathbf{q}})]^{-1}+[\gamma-i(\Delta_\mu+\Delta_{\sigma\mathbf{k}})]^{-1}\}$$
$$-(\gamma-i\Delta_{\mathbf{k}})^{-1}\xi(\Delta_{\mathbf{q}\mu})-(\gamma-i\Delta_{\mathbf{q}})^{-1}\xi(\Delta_{\mathbf{k}\sigma}))\ . \tag{B4}$$

The function $|g_{\mathbf{q}}|^2$ is a slowly varying function and can be evaluated at $\Delta_{\mathbf{q}}=0$. The summation over $\mathbf{q}$ can be converted to an integral and evaluated by contour integration using a representation of the ξ function [19]

$$\xi(x)=i\lim_{\sigma\to 0}(x+i\sigma)^{-1} \tag{B5}$$

[the parameter σ satisfies $\Gamma\gg\sigma\gg t^{-1}$]. Each term in the integrand contains a ξ function, except for one term which varies as

$$\xi(\Delta_{\mathbf{k}\sigma})/(\gamma^2+\Delta_{\mathbf{q}}^2)\ .$$

Although this term is smaller than the others by a factor $(\Gamma t)^{-1}$, its contribution to the *integral* is of the same order since its spectral width is Γt times larger than the width of other terms. After carrying out the summation in (B4), one finds

$$C^{\rm sp}(\mu,\sigma)=-\chi_1\chi_3^*\chi_2 g_{\mathbf{k}}^*\Gamma[(\gamma-i\Delta_1)(\gamma-i\Delta_2)(\gamma+i\Delta_3)]^{-1}$$
$$\times(\xi(\Delta_{3\mu})\xi(\Delta_{\mathbf{k}\sigma})-\xi(\bar{\Delta})\{[\gamma-i(\Delta_1+\Delta_2-\Delta_3)]^{-1}+[\gamma-i(\Delta_1+\Delta_2-\Delta_{\mathbf{k}})]^{-1}\}$$
$$+\xi(\Delta_{\mathbf{k}\sigma})[\Gamma^{-1}-(\gamma-i\Delta_3)^{-1}-(\gamma+i\Delta_\mu)^{-1}]-\xi(\Delta_{3\mu})(\gamma-i\Delta_{\mathbf{k}})^{-1}) \tag{B6}$$

where

$$\Gamma=2\pi\sum_{\mathbf{q}}|g_{\mathbf{q}}|^2\delta(\Delta_{\mathbf{q}}) \tag{B7}$$

and the fact $\Gamma=2\gamma$ was used.

Substituting Eqs. (B3) and (B6) in the formulas (12b) and (12a), one obtains the probability for 4WM emission given by

$$P=\left|\frac{2\chi_1\chi_3^*\chi_2[\Gamma-i(\Delta_3+\Delta_{\mathbf{k}})]}{(\gamma-i\Delta_1)(\gamma-i\Delta_2)(\gamma+i\Delta_3)(\gamma-i\Delta_{\mathbf{k}})}\right|^2$$
$$\times\sum_{\mathbf{k}}A_{\mathbf{k}}|g_{\mathbf{k}}|^2|\xi(\bar{\Delta})|^2\ , \tag{B8}$$

where the $|\xi(\bar{\Delta})|^2$ function has allowed us to set $\bar{\Delta}=0$ in the frequency denominators. This leads to a corresponding emission rate

$$I=I_0\left|2\frac{\chi_1\chi_2\chi_3[\Gamma-i(\Delta_{\mathbf{k}}+\Delta_3)]}{(\gamma-i\Delta_1)(\gamma-i\Delta_2)(\gamma-i\Delta_{\mathbf{k}})(\gamma+i\Delta_3)}\right|^2. \tag{B9}$$

2. Collision-induced extra resonance

The amplitude technique can be also used to establish the origin of so-called pressure-induced extra resonances in 4WM (PIER4) [1]. In considering the pressure-induced extra resonance in three-wave mixing (PIER3), Grynberg and Berman [2] showed that the extra resonance can be linked to processes involving spontaneous emission. As such, this contribution must be calculated "exactly" (beyond the secular approximation), although the limit $|\Delta_i|\gg\gamma$ may be taken in the final result. On the other hand, the stimulated contribution is not sensitive to collisions in the secular approximation.

The situation is not exactly the same for the PIER4 line shape. As in PIER3, one can link the extra resonance to diagrams involving spontaneous emission; however, the diagrams involving spontaneous emission give rise to additional terms. These terms are canceled by corresponding terms in the *stimulated* amplitude, calculated beyond the secular approximation.

Dephasing collisions [20] can be introduced by adding a random function $\delta\omega(t)$ to the frequency of the atomic transition. The previous formulas are modified as

$$\exp(\pm i\Delta_i t)\to\exp\{\pm i[\Delta_i t+\varphi(t)]\}\ , \tag{B10}$$

where $\varphi(t)=-\int_0^t dt'\delta\omega(t')$ is the collision-induced phase shift of the atomic dipole. The function $\delta\omega(t)$ consists of a random series of frequency spikes whose duration τ_c is shorter than all other relevant time scales in the problem. The average time between spikes is the inverse collision rate $1/\gamma'$. Our model is equivalent to that used to derive the corresponding density-matrix equations in the impact limit. All effects related to the velocity-changing aspects of collisions are neglected (the atoms are considered to be stationary).

The expression for the emission probability must be averaged over collision histories using the formula

$$\langle\exp\{\pm i[\varphi(t)-\varphi(t')]\}\rangle_{\rm coll}=\exp[-\gamma'(t-t')]\ , \tag{B11}$$

where $t>t'$. To illustrate the procedure, we consider contribution (d) in Fig. 7, given by

$$\langle \delta P \rangle_{\rm coll} = \left\langle \sum_{\mathbf{k}} \sum_{j,j'} \exp\{i[\bar{\mathbf{k}}\cdot(\mathbf{r}_j - \mathbf{r}_{j'})]\} C_{2\mathbf{k}1}(j) C_3^*(j) C_3(j') C_{2\mathbf{k}1}^*(j') \right\rangle_{\rm coll} .$$

As the averaging for each site j and j' can be carried out independently, one finds

$$\langle \delta P \rangle_{\rm coll} = \sum_{\mathbf{k}} A_{\mathbf{k}} |\langle C_{2\mathbf{k}1} C_3^* \rangle_{\rm coll}|^2 . \tag{B12}$$

Rules (7) and replacements (B10) enable one to write the product of amplitudes in (B12) as

$$C_3^* C_{\sigma\mathbf{k}\mu} = -\chi_1 \chi_3^* \chi_2 g_{\mathbf{k}}^* \int_0^t dt_1 \int_0^{t_1} dt_2 \int_0^{t_2} dt_3 \int_0^t d\tau \, \Phi(t_1,t_2,t_3,\tau) , \tag{B13a}$$

$$\begin{aligned}\Phi(t_1,t_2,t_3,\tau) = {} & \exp[-i(\Delta_\mu t_1 + \varphi(t_1)) - \gamma(t-t_1)] \exp\{i[\Delta_{\mathbf{k}} t_2 + \varphi(t_2)]\} \\ & \times \exp\{-i[\Delta_\sigma t_3 + \varphi(t_3)] - \gamma(t_2 - t_3)\} \exp\{i[\Delta_3 \tau + \varphi(\tau)] - \gamma(t-\tau)\} .\end{aligned} \tag{B13b}$$

To carry out the collisional average one cannot apply formula (B11) since time variables in Eqs. (B13) are not properly time ordered. To overcome this obstacle, the integral equality

$$\begin{aligned}\int_0^t dt_1 \int_0^t dt_2 \cdots \int_0^{t_{n-1}} dt_n \int_0^t d\tau = {} & \int_0^t d\tau \int_0^\tau dt_1 \int_0^{t_1} dt_2 \cdots \int_0^{t_{n-1}} dt_n \\ & + \int_0^t dt_1 \int_0^{t_1} dt_2 \int_0^{t_2} dt_2 \cdots \int_0^{t_{n-1}} dt_n + \cdots + \int_0^t dt_1 \int_0^{t_1} dt_2 \cdots \int_0^{t_{n-1}} dt_n \int_0^{t_n} d\tau\end{aligned}$$

should be used. It enables one to rewrite (B13a) as time-ordered integrals

$$\begin{aligned}C_3^* C_{\sigma\mathbf{k}\mu} = -\chi_1 \chi_3^* \chi_2 g_{\mathbf{k}}^* \Bigg\{ & \Bigg[\int_0^t d\tau \int_0^\tau dt_1 \int_0^{t_1} dt_2 \int_0^{t_2} dt_3 + \int_0^t dt_1 \int_0^{t_1} d\tau \int_0^\tau dt_2 \int_0^{t_2} dt_3 \\ & + \int_0^t dt_1 \int_0^{t_1} dt_2 \int_0^{t_2} d\tau \int_0^\tau dt_3 + \int_0^t dt_1 \int_0^{t_1} dt_2 \int_0^{t_2} dt_3 \int_0^{t_3} d\tau \Bigg] \Phi(t_1,t_2,t_3,\tau) \Bigg\} .\end{aligned}$$

Using formula (B11) to carry out the collisional average, one finds

$$\langle C_3^* C_{\sigma\mathbf{k}\mu} \rangle_{\rm coll} = -\chi_1 \chi_3^* \chi_2 g_{\mathbf{k}}^* [(\bar\gamma - i\Delta_1)(\bar\gamma - i\Delta_2)(\bar\gamma + i\Delta_3)]^{-1} [1 + 2\gamma'/(\Gamma + i\Delta_{3\mu})] \exp(i\Delta_{3\mu} t) \xi(\Delta_{\mathbf{k}\sigma}) ,$$

where $\bar\gamma = \gamma + \gamma'$ is the homogeneous, pressure-broadened width of the transition.

Similar transformations for the other contributions allow one to obtain final expressions for the collisionally averaged, stimulated and spontaneous amplitudes given by

$$\begin{aligned}C^{\rm st}(\mu,\sigma) = {} & \chi_1 \chi_3^* \chi_2 g_{\mathbf{k}}^* [(\bar\gamma - i\Delta_1)(\bar\gamma - i\Delta_2)(\bar\gamma + i\Delta_3)]^{-1} \\ & \times (2\bar\gamma \xi(\Delta_{\mathbf{k}\sigma}) \xi(\Delta_{3\mu}) - \xi(\bar\Delta) \{(\bar\gamma + i\Delta_3)[(\bar\gamma - i\Delta_{\mathbf{k}})^{-1} + (\bar\gamma - i\Delta_3)^{-1}] \\ & \qquad - 2\gamma'(\Gamma + i\Delta_{3\sigma})^{-1} (\bar\gamma - i\Delta_\mu)[(\bar\gamma - i\Delta_{\mathbf{k}})^{-1} + (\bar\gamma + i\Delta_\mu)^{-1}]\} \\ & - \xi(\Delta_{\mathbf{k}\sigma})[1 + (\bar\gamma + i\Delta_3)/(\bar\gamma - i\Delta_3) + (\bar\gamma - i\Delta_\mu)/(\bar\gamma + i\Delta_\mu) + \exp(i\Delta_{3\mu} t) 2\gamma'/(\Gamma + i\Delta_{3\mu})] \\ & - \xi(\Delta_{3\mu})(2\bar\gamma + i\Delta_{3\mu})/(\gamma - i\Delta_{\mathbf{k}})) ,\end{aligned} \tag{B14a}$$

$$\begin{aligned}C^{\rm sp}(\mu,\sigma) = {} & -\chi_1 \chi_3^* \chi_2 g_{\mathbf{k}}^* \Gamma [(\bar\gamma - i\Delta_1)(\bar\gamma - i\Delta_2)(\bar\gamma + i\Delta_3)]^{-1} \\ & \times [\xi(\Delta_{\mathbf{k}\sigma}) \xi(\Delta_{3\mu})[1 + 2\gamma'/(\Gamma + i\Delta_{3\mu})] \\ & - \xi(\bar\Delta)((\bar\gamma - i\Delta_{\mathbf{k}})^{-1} + (\bar\gamma - i\Delta_3)^{-1} + 2(\gamma'/\Gamma)\{(\Gamma + i\Delta_{3\mu})^{-1} + (\bar\gamma - i\Delta_3)^{-1} \\ & \qquad - (\bar\gamma - i\Delta_\mu)/[(\bar\gamma + i\Delta_\mu)(\Gamma + i\Delta_{3\sigma})]\} \\ & \qquad + 2\gamma'/[(\bar\gamma - i\Delta_{\mathbf{k}})(\Gamma + i\Delta_{3\mu})]) \\ & + \xi(\Delta_{\mathbf{k}\sigma})\{\Gamma^{-1} - (\bar\gamma - i\Delta_3)^{-1} - (\bar\gamma + i\Delta_\mu)^{-1} - 2(\gamma'/\Gamma)[(\Gamma + i\Delta_{3\mu})^{-1} \\ & \qquad + (\bar\gamma - i\Delta_3)^{-1} + (\bar\gamma + i\Delta_\mu)^{-1}]\} - \xi(\Delta_{3\mu})(\bar\gamma - i\Delta_{\mathbf{k}})^{-1}[1 + 2\gamma'/(\Gamma + i\Delta_{3\mu})]] .\end{aligned} \tag{B14b}$$

Evaluating these formulas in the secular approximation, i.e., assuming that $\Delta_i \approx \Delta$ $(i=1,2,3)$ and $|\Delta| \gg \Gamma$, but $\delta=\Delta_{31}\approx\Delta_{32}\lesssim\Gamma$, one obtains

$$C^{\mathrm{st}}(\mu,\sigma)=i\chi_1\chi_3^*\chi_2 g_{\mathbf{k}}^*\Delta^{-3} \times\{2\bar{\gamma}\xi(\Delta_{\mathbf{k}\sigma})\xi(\delta)+2\xi(\bar{\Delta}) +\xi(\Delta_{\mathbf{k}\sigma})[1-\exp(i\delta t)2\gamma'(\Gamma+i\delta)^{-1}]\}\ , \tag{B15a}$$

$$C^{\mathrm{sp}}(\mu,\sigma)=-\chi_1\chi_3^*\chi_2 g_{\mathbf{k}}^*\Delta^{-3} \times\{\Gamma\xi(\Delta_{\mathbf{k}\sigma})\xi(\delta)[1+2\gamma'(\Gamma+i\delta)^{-1}] -\xi(\bar{\Delta})4\gamma'(\Gamma+i\delta)^{-1} +\xi(\Delta_{\mathbf{k}\sigma})[1-2\gamma'(\Gamma+i\delta)^{-1}]\}\ . \tag{B15b}$$

Equation (B15) leads to the rate of emission

$$I=I_0\left|4\frac{\chi_1\chi_3^*\chi_2}{\Delta^3}\left[1+\frac{2\gamma'}{\Gamma+i\delta}\right]\right|^2 ,$$

which is the well known result [1] for the pressure induced resonance.

3. Doppler-broadened recoil-induced line

We showed in Sec. II that, to obtain the RIR, it is sufficient to calculate the amplitudes to order Δ_i^{-2}. The corresponding calculation for arbitrary ratios of Δ_i to Γ is zeroth order in the parameter $(\gamma t)^{-1}$. This simplification actually makes the amplitude technique even easier than the density-matrix approach used previously [3].

Consider, for example, the four-photon amplitude (35). One can set the lower limits of integration over t_2 and t_4 equal $-\infty$ and obtain the formula

$$C_{\mu 3\sigma\mathbf{k}}(\mathbf{p})=\chi_1\chi_3^*\chi_2 g_{\mathbf{k}}^*\xi(\tilde{\Delta}_{\mathbf{k}\sigma}-\omega_{3\mu},\tilde{\Delta}_{3\mu}+\omega_{3\mu}) \times\{[\gamma-i(\Delta_\sigma-\omega_{\mathbf{p}+\hbar\mathbf{k},\mathbf{p}+\hbar(\mathbf{k}-\mathbf{k}_\sigma)})] \times[\gamma-i(\Delta_\mu-\omega_{\mathbf{p}+\hbar\mathbf{k}_\mu,\mathbf{p}})]\}^{-1}\ , \tag{B16}$$

where the momentum conservation law (1a) was used and the function $\xi(\Delta,\Delta')$ is defined by Eq. (15b). Similar calculations lead to the two-quantum amplitude

$$C_{\alpha\beta}(\mathbf{p})=-\chi_\alpha\chi_\beta^*\xi(\tilde{\Delta}_{\beta\alpha}+\omega_{\beta\alpha}) \times[\gamma-i(\Delta_\alpha-\omega_{\mathbf{p}+\hbar\mathbf{k}_\alpha,\mathbf{p}})]^{-1}\ . \tag{B17}$$

Substituting these results in (12c) one arrives at the stimulated amplitude

$$\begin{aligned}C^{\mathrm{st}}(\mu,\sigma;\mathbf{p})=\chi_1\chi_3^*\chi_2 g_{\mathbf{k}}^*\int_0^t dt'\xi(\bar{\Delta},t,t')(&\exp[-i(\tilde{\Delta}_{3\mu}+\omega_{3\mu})t'] \\ &\times\{[\gamma-i(\Delta_\sigma-\omega_{\mathbf{p}+\hbar\mathbf{k},\mathbf{p}+\hbar(\mathbf{k}-\mathbf{k}_\sigma)})][\gamma-i(\Delta_\mu-\omega_{\mathbf{p}+\hbar\mathbf{k}_\mu,\mathbf{p}})]\}^{-1} \\ &+\exp[-i(\tilde{\Delta}_{3\mu}-\omega_{3\mu})t'][\gamma-i(\Delta_\sigma-\omega_{\mathbf{p}+\hbar\mathbf{k}_\sigma,\mathbf{p}})] \\ &\qquad\times[\gamma+i(\Delta_3-\omega_{\mathbf{p}+\hbar\mathbf{k}_3,\mathbf{p}})]\}^{-1} \\ &+\exp[-i(\tilde{\Delta}_{\mathbf{k}\sigma}+\omega_{3\mu})t'][\gamma-i(\Delta_\sigma-\omega_{\mathbf{p}+\hbar\mathbf{k}_\sigma,\mathbf{p}})]^{-1} \\ &\times\{[\gamma-i(\Delta_\mu-\omega_{\mathbf{p}+\hbar\mathbf{k}_3,\mathbf{p}+\hbar\mathbf{k}_{3\mu}})]^{-1} \\ &\quad+[\gamma+i(\Delta_3-\omega_{\mathbf{p}+\hbar\mathbf{k}_3,\mathbf{p}})]^{-1}\})\ ,\end{aligned} \tag{B18}$$

where Eqs. (18), (40c), and the relation $\xi(\Delta,\Delta')=\int_0^t dt'\xi(\Delta+\Delta',t,t')\exp(-i\Delta' t')$ were used. The third summand in (12c) was omitted, since it does not contribute to this order.

To calculate the spontaneous amplitude

$$C^{\mathrm{sp}}(\mu,\sigma,\mathbf{p})=\sum_{\mathbf{q}}[C_{\mu q\sigma\mathbf{k}}(\mathbf{p})+C_{\sigma\mathbf{k}\mu q}(\mathbf{p})]C_{3q}^*(\mathbf{p})\ , \tag{B19}$$

one cannot use the previous formula since $\mathbf{q}\neq\mathbf{k}+\mathbf{k}_\sigma-\mathbf{k}_\mu$. To calculate $C^{\mathrm{sp}}(\mu,\sigma,\mathbf{p})$ one returns to the integral form (35) and carries out the summation over $\mathbf{q}$ to obtain

$$\begin{aligned}C^{\mathrm{sp}}(\mu,\sigma;\mathbf{p})=-\chi_1\chi_3^*\chi_2 g_{\mathbf{k}}^*\Gamma\int_0^t dt'\xi(\bar{\Delta},t,t')(&\exp[-i\tilde{\Delta}_{\mathbf{k}\sigma}+\omega_{3\mu})t'] \\ &\times\{[\gamma+i(\Delta_3-\omega_{\mathbf{p}+\hbar\mathbf{k}_3,\mathbf{p}})][\gamma-i(\Delta_\sigma-\omega_{\mathbf{p}+\hbar\mathbf{k}_\sigma,\mathbf{p}})] \\ &\quad\times[\gamma-i(\Delta_\mu-\omega_{\mathbf{p}+\hbar\mathbf{k}_3,\mathbf{p}+\hbar\mathbf{k}_{3\mu}})]\}^{-1} \\ &+\{[\gamma-i(\Delta_\mu-\omega_{\mathbf{p}+\hbar\mathbf{k}_\mu,\mathbf{p}})][\gamma+i(\Delta_3-\omega_{\mathbf{p}+\hbar\mathbf{k}_3,\mathbf{p}})]\}^{-1} \\ &\quad\times\int d\mathbf{n}_{\mathbf{q}}N_{\mathbf{q}}\exp[-i(\tilde{\Delta}_{3\mu}+\omega_{\mathbf{k}_\mu-\mathbf{q}}-\omega_{\mathbf{k}_3-\mathbf{q}})t'] \\ &\qquad\times[\gamma-i(\Delta_\sigma-\omega_{\mathbf{p}+\hbar(\mathbf{k}_\mu+\mathbf{k}_\sigma-\mathbf{q}),\mathbf{p}+\hbar(\mathbf{k}_\mu-\mathbf{q})})]^{-1})\ ,\end{aligned} \tag{B20}$$

where $\mathbf{n}_q=\mathbf{q}/q$ and

$$N_{\mathbf{q}}=|g_{\mathbf{q}}|^2\Big/\int d\mathbf{n}_q|g_{\mathbf{q}}|^2 \ . \tag{B21}$$

After some algebraic manipulations, one can combine (B18) and (B20) to reach the total amplitude (33)

$$C(\mu,\sigma;\mathbf{p})=g_{\mathbf{k}}^*\int_0^t d\tau\,\xi(\bar{\Delta},t,\tau)[R_{\mu\sigma}(\tau)+r_{\mu\sigma}(\tau)] \ , \tag{B22a}$$

where

$$\begin{aligned}R_{\mu\sigma}(\tau)=\chi_1\chi_3^*\chi_2(&\exp[-i(\tilde{\Delta}_{3\mu}+\omega_{3\mu})\tau]\{[\gamma-i(\Delta_\sigma-\omega_{\mathbf{p}+\hbar\mathbf{k},\mathbf{p}+\hbar(\mathbf{k}-\mathbf{k}_\sigma)})][\gamma-i(\Delta_\mu-\omega_{\mathbf{p}+\hbar\mathbf{k}_\mu,\mathbf{p}})]\}^{-1}\\
&+\exp[-i(\tilde{\Delta}_{3\mu}-\omega_{3\mu})\tau]\{[\gamma+i(\Delta_3-\omega_{\mathbf{p}+\hbar\mathbf{k}_3,\mathbf{p}})][\gamma-i(\Delta_\sigma-\omega_{\mathbf{p}+\hbar\mathbf{k}_\sigma,\mathbf{p}})]\}^{-1}\\
&-\{[\gamma-i(\Delta_\mu-\omega_{\mathbf{p}+\hbar\mathbf{k}_\mu,\mathbf{p}})][\gamma+i(\Delta_3-\omega_{\mathbf{p}+\hbar\mathbf{k}_3,\mathbf{p}})]\}^{-1}\\
&\times\Gamma\int d\mathbf{n}_q N_{\mathbf{q}}\exp[-i(\tilde{\Delta}_{3\mu}+\omega_{\mathbf{k}_\mu-\mathbf{q}}-\omega_{\mathbf{k}_3-\mathbf{q}})\tau][\gamma-i(\Delta_\sigma-\omega_{\mathbf{p}+\hbar(\mathbf{k}_\mu+\mathbf{k}_\sigma-\mathbf{q}),\mathbf{p}+\hbar(\mathbf{k}_\mu-\mathbf{q})}]^{-1})\ ,\end{aligned} \tag{B22b}$$

and

$$\begin{aligned}r_{\mu\sigma}(\tau)=&i\chi_1\chi_3^*\chi_2[\bar{\Delta}-(\tilde{\Delta}_{\mathbf{k}\sigma}+\omega_{3\mu})]\exp[-i(\tilde{\Delta}_{\mathbf{k}\sigma}+\omega_{3\mu})\tau]\\
&\times\{[\gamma+i(\Delta_3-\omega_{\mathbf{p}+\hbar\mathbf{k}_3,\mathbf{p}})][\gamma-i(\Delta_\sigma-\omega_{\mathbf{p}+\hbar\mathbf{k}_\sigma,\mathbf{p}})][\gamma-i(\Delta_\mu-\omega_{\mathbf{p}+\hbar\mathbf{k}_3,\mathbf{p}+\hbar\mathbf{k}_{3\mu}})]\}^{-1} \ .\end{aligned} \tag{B22c}$$

The exponential in (B22c) restricts $|\tilde{\Delta}_{\mathbf{k}\sigma}+\omega_{3\mu}|\lesssim 1/\tau\sim 1/t$. Since the ξ function in (B22a) restricts $\bar{\Delta}\lesssim 1/t$, one estimates that $r_{\mu\sigma}(t)\sim(\gamma t)^{-1}R_{\mu\sigma}(t)$. It also follows that the classical limit of Eq. (B22b)

$$R^0_{\mu\sigma}(\tau)=R_{\mu\sigma}(\tau)|_{\hbar\to 0}=i\chi_1\chi_3^*\chi_2\bar{\Delta}_{3\mu}\exp(-i\tilde{\Delta}_{3\mu}\tau)[(\gamma-i\tilde{\Delta}_\sigma)(\gamma-i\tilde{\Delta}_\mu)(\gamma+i\tilde{\Delta}_3]^{-1} \tag{B23}$$

is $(\gamma t)^{-1}$ times smaller than $R_{\mu\sigma}(\tau)$, implying that only quantum corrections to the amplitudes play an essential role in 4WM to zeroth order in $(\Gamma t)^{-1}$. Omitting the remainder $r_{\mu\sigma}(\tau)$ in (B22a), but for convenience, subtracting off a (negligible) contribution $R^0_{\mu\sigma}(\tau)$ from (B22b), one can write

$$C(\mu,\sigma;\mathbf{p})=g_{\mathbf{k}}^*\int_0^t d\tau\,\xi(\bar{\Delta},t,\tau)[R_{\mu\sigma}(\tau)-R^0_{\mu\sigma}(\tau)] \ . \tag{B24}$$

Following the same path that took us from Eq. (40a) to Eqs. (43), we arrive at Eqs. (64) of the text.

---

[1] For reviews of this subject area, see L. Rothberg, in *Progress in Optics,* edited by E. Wolf (Elsevier Scientific, Amsterdam, 1987), pp. 39–101; G. Grynberg, in *Spectral Line Shape,* edited by R. Exton (Deepak, Hampton, VA, 1987), Vol. 4, pp. 503–521; G. S. Agarwal, in *Advances in Atomic and Moelcular Physics,* edited by D. Bates and B. Bederson (Academic, New York, 1992), pp. 113–176.

[2] G. Grynberg and P. R. Berman, Phys. Rev. A **43**, 3994 (1991).

[3] J. Guo, P. R. Berman, B. Dubetsky, and G. Grynberg, Phys. Rev. A **46**, 1426 (1992).

[4] See, for example, Y. Prior, A. R. Bogdan, M. Dagenais, and N. Bloembergen, Phys. Rev. Lett. **46**, 111 (1981).

[5] P. R. Berman and G. Grynberg, Phys. Rev. A **39**, 570 (1989).

[6] P. R. Berman, G. Khitrova, and J. Lam, in *Spectral Line Shapes,* edited by F. Rostas (deGruyter, Berlin, 1985), Vol. 3, pp. 337 and 338.

[7] See, for example, C. Cohen-Tannoudji, J. Dupont-Roc, and G. Grynberg, *Atom-Photon Interactions* (Wiley, New York, 1992), Chap. 6.

[8] M. Gorlicki, P. R. Berman, and G. Khitrova, Phys. Rev. A **37**, 4340 (1988).

[9] The spontaneous term can be calculated in the secular approximation without the need of going to the "exact" equations of Appendix B. If the amplitude is written in integral form and the sum on **q** carried out, the resulting expression can be evaluated directly in the secular approximation.

[10] P. R. Berman and G. Grynberg, Phys. Rev. A **40**, 6921 (1989).

[11] In the momentum representation, the function $A_{\mathbf{k}}$ should be replaced by $A'_{\mathbf{k}}=N^2\delta(\bar{\mathbf{k}})$; however, since both $A_{\mathbf{k}}$ and $A_{\mathbf{k}'}$ lead to the same final line shape, we have not distinguished between them in the text.

[12] *Handbook of Mathematical Functions,* edited by M. Abramowitz and I. A. Stegun, Natl. Bur. Stand. Appl. Math. Ser. No. 55, U.S. GPO, Washington, DC 1964), Eq. 7.1.3.

[13] The background is proportional to $\xi(\bar{\Delta})$ while the RIR amplitude term is proportional to $\xi(\bar{\Delta},t,t')$. It is possible to show that the signal can still be written in the form (64) with $S(t)=\sum_{\mu(\neq\sigma)}[S_{\mu\sigma}(t)-S^0_{\mu\sigma}(t)]+S_{bck}$.

[14] See, for example, M. S. Feld and A. Javan, Phys. Rev. **177**, 549 (1969).

[15] It is implicitly assumed that the atoms act as free particles and interact with the fields for time t. For cold atoms ($ku\ll\gamma$), an upper limit on t is provided by the time it takes an atom to diffuse out of the interaction volume as a result of heating by the fields. Atomic localization effects, which can also lead to narrow resonances, are not considered in this work. See, for example, P. Verkerk, B. Lounis, C. Salomon, C. Cohen-Tannoudji, J.-Y. Courtois, and G. Grynberg, Phys. Rev. Lett. **68**, 3861 (1992); P. S.

Jessen, C. Gerz, P. D. Lett, W. D. Phillips, S. L. Rolston, R. J. C. Spreeuw, and C. I. Westbrook, *ibid.* **69**, 49 (1992).

[16] See, for example, P. R. Berman, D. J. Steel, G. Khitrova, and J. L. Liu, Phys. Rev. A **38**, 252 (1988).

[17] G. Grynberg and C. Cohen-Tannoudji (unpublished). We are grateful to Professor Grynberg and Professor Cohen-Tannoudji for a copy of their article prior to publication.

[18] See, for example, A. M. Levine, N. Chencinski, W. M. Schreiber, A. N. Weiszmann, and Y. Prior, Phys. Rev. A **35**, 2550 (1987).

[19] W. Heitler, *The Quantum Theory of Radiation,* 3rd ed. (Oxford University Press, London, 1954), Sec. II.8.

[20] The collision-induced resonances are calculated in the stationary atom approximation. If the calculation is generalized to allow for atomic motion, then velocity-changing collisions can affect atomic state populations and lead to modified line shapes (see Ref. [8]).